JOURNAL OF GEOPHYSICAL RESEARCH, VOL. 87, NO. B6, PAGES 4761-4784, JUNE 10, 1982

URANIUM-LEAD ISOTOPIC AGES FROM THE SIERRA NEVADA BATHOLITH, CALIFORNIA

James H. Chen[1]

Department of Geological Sciences, University of California
Santa Barbara, California 93106

James G. Moore

U.S. Geological Survey, Menlo Park, California 94025

Abstract. This study provides new information on the timing and distribution of Mesozoic magmatic events in the Sierra Nevada batholithic complex chiefly between 36° and 37°N. latitude. U-Pb ages have been determined for 133 zircon and 7 sphene separates from 82 samples of granitoid rocks. Granitoid rocks in this area range in age from 217 to 80 m.y. Triassic intrusions are restricted to the east side of the batholith; Jurassic plutons occur south of the Triassic plutons east of the Sierra Nevada, as isolated masses within the Cretaceous batholith, and in the western foothills of the range; Cretaceous plutons form a continuous belt along the axis of the batholith and occur as isolated masses east of the Sierra Nevada. No granitic intrusions were emplaced for 37 m.y. east of the Sierra Nevada following the end of Jurassic plutonism. However, following emplacement of the eastern Jurassic granitoids, regional extension produced a fracture system at least 350 km long into which the dominantly mafic, calc-alkalic Independence dike swarm was intruded 148 m.y. ago. The dike fractures probably represents a period of regional crustal extension caused by a redistribution of the regional stress pattern accompanying the Nevadan orogeny. Intrusion of Cretaceous granitic plutons began in large volume about 120 m.y. ago in the western Sierra Nevada and migrated steadily eastward for 40 m.y. at a rate of 2.7 mm/y. This slow and constant migration indicates remarkably uniform conditions of subduction with perhaps downward migration of parent magma generation or a slight flattening of the subduction zone. Such steady conditions could be necessary for the production of large batholithic complexes such as the Sierra Nevada. The abrupt termination of plutonism 80 m.y. ago may have resulted from an increased rate of convergence of the American and eastern Pacific plates and dramatic flattening of the subduction zone. U-Pb ages of the Giant Forest-alaskite sequence in Sequoia National Park are all in the range 99 ± 3 m.y., indicating a relatively short period of emplacement and cooling for this nested group of plutons. U-Pb ages of a mafic inclusion and its host granodiorite indicate that both were derived from a common source or that the mafic inclusion was totally equilibrated with the granodioritic magma. Comparison of isotopic ages determined by different methods such as zircon U-Pb, sphene U-Pb, hornblende K-Ar, and biotite K-Ar suggests that zircon U-Pb ages generally approximate the emplacement age of a pluton. However, some plutons probably contain inherited or entrained old zircons, and the zircons of some samples are disturbed by younger thermal and metamorphic events. The ages reported here are consistent with U-Pb age determinations previously made on granitic rocks to the north [Stern et al., 1981]. The age distribution of granitic belts determined here is in general agreement with those established by K-Ar dating [Evernden and Kistler, 1970] but does not differentiate the five epochs of plutonism determined in their study.

Introduction

The Mesozoic Sierra Nevada batholith of California (Figure 1) is part of a more or less continuous belt of Mesozoic plutonic rocks along the western margin of North America. The large composite batholith provides an excellent testing ground for models of magma genesis and mechanism of emplacement [Bateman and Wahrhaftig, 1966; Bateman and Eaton, 1967; Hamilton, 1969; Kistler et al., 1971; Shaw et al., 1971; Kistler, 1974]. Many lines of evidence, including initial $^{87}Sr/^{86}Sr$ values [Kistler et al., 1971; Kistler and Peterman, 1973; Kistler, 1974], K_2O content [Bateman and Dodge, 1970], quartz diorite boundary line [Moore, 1959], rare-earth element pattern and content [Dodge and Mays, 1972], and lead isotopic composition [Doe and Delevaux, 1973], suggest a source region that was laterally variable in composition both along and across strike. An understanding of these geochemical and geophysical variations requires knowledge of the age distribution of granitic plutonism. The present investigation provides new age data principally between 36° and 37° north latitude.

Most of the available ages determined for granitic rocks of the Sierra Nevada batholith and adjacent areas are by the K-Ar method on mineral separates. Additional dates have been determined by the U-Pb technique on accessory zircon or by the Rb-Sr whole-rock technique. Kistler et al. [1965], Kistler and Dodge [1966], and Evernden and Kistler [1970] reported many K-Ar dates of minerals, principally biotite and hornblende, from plutons in California and Nevada. Subsequent geochronological studies in

---

[1]Now at Division of Geological and Planetary Sciences, California Institute of Technology, Pasadena, California 91125

Paper number 2B0361.
0148-0227/82/002B-0361$05.00

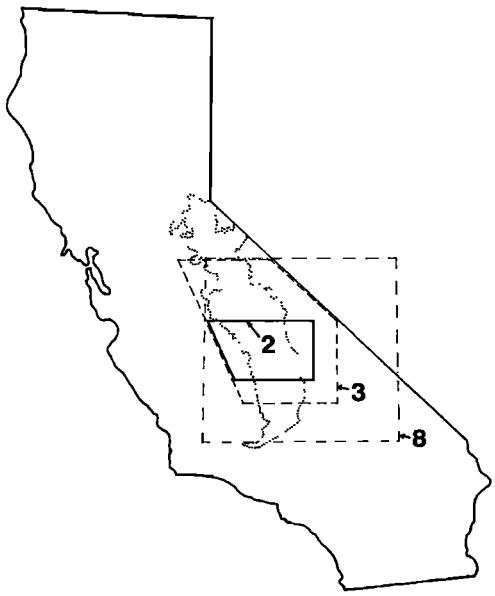

Fig. 1. Index map of California showing Sierra Nevada batholith (dotted outline) and areas of Figures 2, 3, and 8.

the North American Cordillera by the K-Ar technique have been made in northwestern Nevada [Smith et al., 1971], in north-central Nevada [Silberman and McKee, 1971a, b], in the White Mountain area [Crowder et al., 1973], and in Nevada, Utah, and southern California [Armstrong and Suppe, 1973] and in Baja California [Krummenacher et al., 1975]. Lanphere and Reed [1973] and Kistler [1974] have analyzed the existing K-Ar data on Mesozoic magma generation and emplacement in western North America.

Since relatively low temperature during metamorphism can expel accumulated radiogenic argon from biotite (210° to 430°C) and hornblende (450° to 500°C) during a short interval of geologic time [Hart, 1964], K-Ar ages may not record the time of primary crystallization. On the other hand, zircons are nearly always able to retain at least part of their radiogenic lead under near-melting conditions [Hart et al., 1968; Chen and Moore, 1979]. Even with substantial loss of lead during metamorphism, the concordia diagram indicates the primary crystallization age of the zircon if the time of metamorphism can be determined from the lead data or by other means [Wetherill, 1956]. Zircon U-Pb dates may therefore indicate the emplacement age of a pluton, whereas K-Ar dates may record only a 'cooling age' or the age of a reheating event of the pluton. In addition, the data of this report indicate complexities in the U-Pb systematics of different size fractions of zircons from some granitic rocks that make precise interpretation of emplacement ages difficult to determine.

Recently, Stern et al. [1981] have reported U-Pb ages on zircons from plutons of the central part of the Sierra Nevada batholith between latitude 37° and 38°N. Their results are generally consistent with the distribution of Cretaceous, Jurassic, and Triassic plutonic belts of Evernden and Kistler [1970]. K-Ar dating of biotite-hornblende pairs, Rb-Sr whole rock dating [Evernden and Kistler, 1970; Kistler et al., 1965], and the data of Stern et al. [1981] indicate that many of the K-Ar ages on biotite and to a lesser degree hornblende from older granitoids have been reduced as a result of reheating by younger plutons.

This report presents the results of U-Pb age determinations from granitic rocks of the Sierra Nevada batholith between latitude 36° and 37° and adjacent area (Figures 2 and 3). Although individual plutons have been mapped only in parts of this area, the results refine and extend our knowledge of the distribution of Sierra Nevada plutonism in space and time.

The Sierra Nevada Batholith

The Sierra Nevada batholith intruded Precambrian, Paleozoic, and early Mesozoic strata which are preserved as the wall rocks, roof pendants, and inclusions within the batholith [Bateman and Wahrhaftig, 1966]. The batholith is composed chiefly of quartz-bearing granitoid rocks ranging in composition from quartz diorite to alaskite with smaller masses of mafic plutonic rocks that include diorite, quartz diorite, and hornblende gabbro.

The granitic batholith can be divided into separate plutons on the basis of similarities in texture, color index, intrusive relations, composition, and other field criteria. The plutons were emplaced as discrete masses which are in sharp contact with one another or are separated by thin septa of metamorphic rocks. Most plutons are elongate in a north-northwesterly direction parallel with the long axis of the batholith, but a few small plutons are elongate in other directions or are rounded in shape.

Intrusive relations define the relative age of plutons in contact. However, correlations in some areas are not complete because of lack of mapping, and even in well-studied areas, a complete intrusive sequence among all the mapped plutons cannot be established because many plutons are not in contact with one another or the contacts are nondiagnostic for relative age determination. Some plutons are nested with the older and more mafic members on the border and younger and more silicic ones in the central area. Many individual plutons are zoned from a silicic core to a mafic border.

Analytical Methods

Eighty-two samples of granitic rocks from the Sierra Nevada batholith were collected and analyzed. Sample descriptions and localities appear in appendix Table A1 and Figures 2 and 3. The samples were crushed, and zircon and sphene were separated by the usual Wilfley table, heavy liquid, and magnetic separation methods. Nonmagnetic zircons were split into three size fractions, -325 (fine), +325-200 (medium), and +200 (coarse) mesh. Zircon and sphene samples, weighing about 10 mg and 50 mg, respectively, were purified by handpicking to at least 99.9% purity. After a final washing in hot 8M HNO_3, the sample was dissolved in HF at

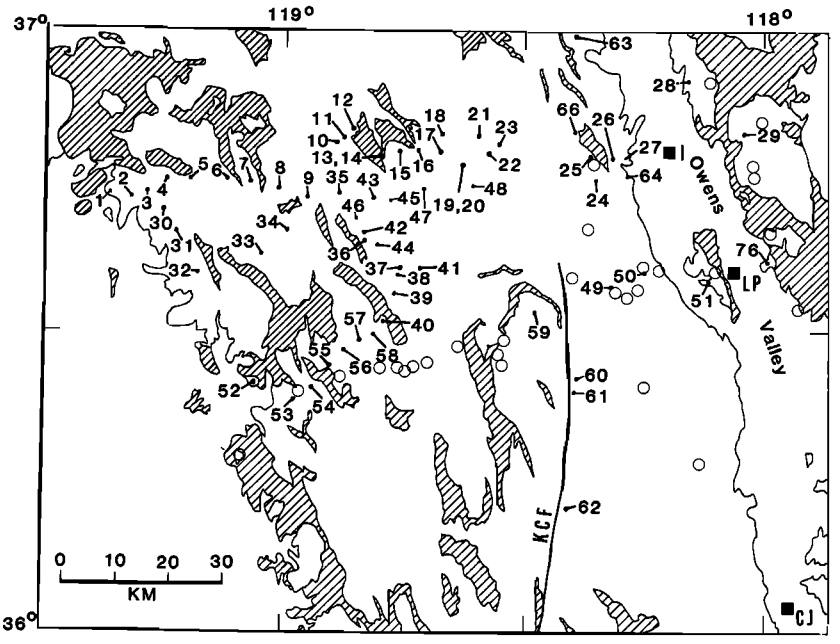

Fig. 2. Map of Sierra Nevada batholith between latitudes 36° and 37° showing the location of most granitic rocks dated in this study. Samples are described in Tables 1 and 2. Open circles are K-Ar sample localities of Evernden and Kistler [1970]. Diagonal pattern, pregranitic rock. Symbols: I, Independence; LP, Lone Pine; CJ, Coso Junction; KCF, Kern Canyon fault.

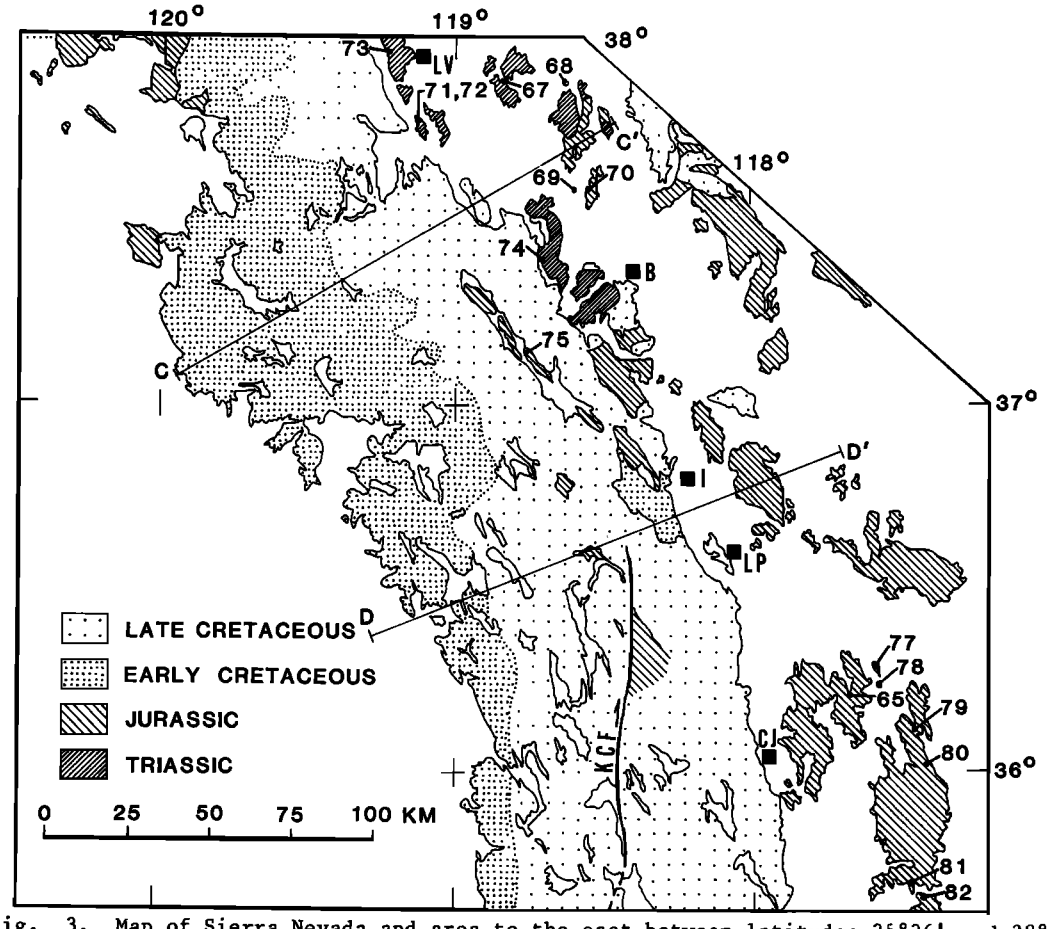

Fig. 3. Map of Sierra Nevada and area to the east between latitudes 35°36' and 38° showing locations of dated granitic samples not shown in Figure 2 and generalized age of granitic rocks. Symbols: LV, Lee Vining; B, Bishop; I, Independence, LP, Lone Pine; CJ, Coso Junction; KCF, Kern Canyon fault.

200°C in a pressured capsule [Krogh, 1973]. At the early stage of this work, a mixed ^{208}Pb–^{235}U spike was added to the sample prior to dissolution to determine the concentration of U and Pb (method s, Table 1). An unspiked aliquot run was necessary to determine the $^{208}Pb/^{206}Pb$ ratio for the isotope dilution calculation. The use of a ^{205}Pb–^{235}U spike at the later stage of this work obviated the need for later aliquoting (method t, Table 1). Chemical purification of U and Pb followed the procedure of Krogh [1973], and was similar to that of Saleeby and Sharp [1980] (for details see Chen 1977]. Lead isotopic composition was measured by mass spectrometry with the silica gel phosphoric acid method, and uranium by the phosphoric acid-graphite method. Lead data were corrected for instrumental mass fractionation of 0.1 ± 0.03% per mass unit based on replicate analyses of U.S. National Bureau of Standard (NBS) Pb standards; uranium data were corrected for 0.1 ± 0.2% per mass unit on the basis of replicate analyses of NBS U standards. The major Pb isotopes (^{208}Pb, ^{207}Pb, and ^{206}Pb) generally produced ion currents of 3×10^{-12} to 2×10^{-11} A for a period of several hours and were measured with a Faraday cup collector. A minor isotope, ^{204}Pb was measured mainly with the electron multiplier when the $^{206}Pb/^{204}Pb$ ratio was high (greater than 200).

Concordancy of U-Pb Ages

The analytical data and calculated ages for 82 granitic rocks from the Sierra Nevada batholith are listed in Tables 1 and 2 and localities are described in the appendix. From one to five fractions of zircon were analyzed, and one fraction of sphene was analyzed for seven samples. The resulting 140 ages shown in Table 1 indicate that many (~40%) of the individual analyses have discordant $^{206}Pb/^{238}U$ and $^{207}Pb/^{235}U$ ages (internal discordancy) and that different zircon size fractions and sphene crystals from the same sample yield somewhat different ages (external discordancy).

Internal Concordancy

The following discussion illustrates the procedures for the estimation of analytical errors in the calculated U-Pb ages. The U-Pb age T calculated for a sample from closed-system decay of ^{238}U to ^{206}Pb is

$$T = \frac{1}{\lambda}\left[\ln\left(1 + \frac{x}{y}\right)\right] \qquad (1)$$

where $x = {}^{206}Pb^{*}$(radiogenic), $y = {}^{238}U$ and $\lambda = 1.55125 \times 10^{-10} y^{-1}$ (Jaffey et al., 1971).

The errors in (1) are related as

$$\sigma_T^2 = \left(\frac{-T}{\lambda}\right)^2 \sigma_\lambda^2 + \left[\frac{1}{y^2}\sigma_x^2 + \left(\frac{-x}{y^2}\right)^2 \sigma_y^2\right] \Big/ \lambda^2 \left(1 + \frac{x}{y}\right)^2 \qquad (2)$$

Similar equations can be given for the ^{235}U–^{207}Pb system. The errors $\sigma\lambda/\lambda$ for decay constants of ^{238}U and ^{235}U are 0.054% and 0.068%, respectively [Jaffey et al., 1971], which are small compared with the errors for the concentrations of radiogenic Pb and U. The value of radiogenic Pb is equal to

$$x = u\,(1 - vw) \qquad (3)$$

where u = total ^{206}Pb, $v = (^{204}Pb/^{206}Pb)_p$ = present ratio, and $w = (^{206}Pb/^{204}Pb)_o$ = initial ratio.

The errors in (3) are related as

$$\sigma_x^2 = (1 - vw)^2 \sigma_u^2 + [u(-w)]^2 \sigma_v^2 + [u(-v)]^2 \sigma_w^2 \qquad (4)$$

The uncertainties in measuring the amounts of U and Pb in a sample are determined by the uncertainties in the U-Pb spike concentrations and the U and Pb isotopic ratios. Since the mixed U-Pb spikes were used, the uncertainty in the weight of either the sample (0.01 to 0.05 g) or the spike (0.1 to 0.5 g) are not significant. The U and Pb concentrations in the spikes determined by isotope dilution with U and Pb standards were precise to 0.3% and 0.1%, respectively [Chen, 1977]. Since the uncertainties in the $^{238}U/^{235}U$ and $^{208}Pb/^{206}Pb$ (or $^{205}Pb/^{206}Pb$) ratios are generally better than 0.2% and 0.1%, respectively, the uncertainties in measuring the amounts of U and Pb are estimated at 0.5% ($\sigma y/y$) and 0.2% ($\sigma u/u$), respectively. In general, the Pb isotopic compositions determined from feldspar or whole rock (corrected for in situ decay of U and Th) [Chen and Tilton, 1978; and unpublished data, 1982] of the same sample analyzed for zircon or sphene are used as 'initial' Pb (w) in (3) and (4). In a few cases, where 'initial' Pb data are not available, the measured Pb isotopic composition of a blank (footnote, Table 1) was used for nonradiogenic Pb correction. The values of $^{206}Pb/^{204}Pb$, $^{207}Pb/^{204}Pb$, and $^{208}Pb/^{204}Pb$ for the common Pb determined for the Sierra Nevada granitoids (70 analyses) range from 18.2 to 19.5, 15.54 to 15.76, and 38.52 to 39.17, respectively [Chen and Tilton, 1978; and unpublished data, 1982]. These values are within ±3%, ±1%, and ±1% of the $^{206}Pb/^{204}Pb$, $^{207}Pb/^{204}Pb$ and $^{208}Pb/^{204}Pb$ ratios, respectively, determined from the Pb blank. The measured Pb blank ranges from 0.2 to 1.5 ng during the period of this work, which can account for at most 50% of the common Pb in the samples. The common Pb is probably present in the samples on the surface or in inclusions or fractures.

In this study, most zircons have $^{204}Pb/^{206}Pb$ less than 10^{-3} (Table 1), and therefore the uncertainty due to nonradiogenic Pb correction is small. For example, sample 1 (Table 1) has a $^{206}Pb/^{204}Pb$ and $^{207}Pb/^{204}Pb$ ratio of 1515 and 88, respectively. Taking the uncertainties of 1% ($\sigma v/v$) for these ratios, of 0.5% ($\sigma y/y$) and 0.2% ($\sigma u/u$) for the U and Pb concentrations, and of 1% ($\sigma w/w$) for the 'initial' Pb isotopic compositions, the uncertainties for the concentration of radiogenic Pb (x) and for the ^{206}Pb–^{238}U age (T) can be calculated from (4) and (2), respectively. The results for sample 1 are 0.6 m.y., 0.7 m.y., and 12 m.y. for the $^{206}Pb/^{238}U$, $^{207}Pb/^{235}U$, and

TABLE 1. Zircon and sphene U-Pb ages

Sample	Field	Concentration, ppm		Isotopic Composition			Age, m.y.		
				^{204}Pb	^{207}Pb	^{208}Pb	$^{206}Pb^*$	$^{207}Pb^*$	$^{207}Pb^*$
		^{238}U	$^{206}Pb^*$	^{206}Pb	^{206}Pb	^{206}Pb	^{238}U	^{235}U	$^{206}Pb^*$
1	W10(m)t	176	2.72	0.00066	0.05806	0.20525	114.2	114.1	113
2	W12(m)t	178	2.69	0.00115	0.06515	0.19834	111.7	111.6	111
3	W22(m)t	223	3.32	0.00066	0.05824	0.24428	110.8	111.4	125
4	W21(c)t	260	3.95	0.00007	0.05084	0.14942	111.9	115.4	188
	(m)t	793	10.74	0.00035	0.05440	0.17324	100.2	102.7	162
5	W5(c)t	543	9.99	0.00031	0.05392	0.13304	135.7	137.2	164
	(m)s	531	10.46	0.00083	0.06145	0.14300	145.2	146.2	163
6	W4(c)s	961	14.44	0.00046	0.05510	0.06788	111.0	111.1	112
7	W3(c)s	434	6.57	0.00047	0.05529	0.10079	111.8	112.0	116
8	W2(f)s	1768	25.43	0.00408	0.10856	0.23654	106.3	106.9	121
9	W6(m)s	2802	48.84	0.00020	0.05145	0.07159	128.6	128.4	124
10	KC11(m)s	716	10.88	0.00062	0.05743	0.25560	112.2	112.3	115
	(f)s	1100	16.36	0.00036	0.05430	0.17936	109.9	111.6	148
11	KC6(c)s	860	12.97	0.00010	0.05011	0.09682	111.5	112.4	130
	(m-1)s	1236	18.23	0.00012	0.05084	0.09563	109.0	110.9	152
	(m-2)s	1219	17.98	0.00013	0.05045	0.09885	109.0	109.8	127
12	KC19(n)t	5894	68.67	0.00043	0.05396	0.22137	86.2	86.1	83
13	KC18(m)s	886	13.83	0.00017	0.05146	0.17042	115.7	117.2	149
14	KC5(m)s	1076	14.43	0.00021	0.05120	0.14600	99.1	99.4	105
15	KC16(m)s	897	13.24	0.00111	0.06451	0.36616	108.0	107.9	106
16	KC2(m)s	1378	19.22	0.00049	0.05499	0.28196	103.9	103.2	90
	(sp)s	223	2.95	0.00750	0.15800	0.91958	97.6	97.3	88
17	KC15(m)s	1804	23.76	0.00019	0.05078	0.17417	97.4	97.3	96
18	68M91(n)s	703	8.87	0.00092	0.06295	0.23795	92.7	95.7	170
	(sp)s	113	1.35	0.01689	0.29584	1.7193	88.7	88.6	86
19	KC14(c)s	3480	60.56	0.00039	0.05458	0.13016	127.6	128.1	137
	(m)s	2766	46.18	0.00077	0.06003	0.15490	119.5	120.0	128
20	KC22(m)s	2351	42.70	0.00014	0.05096	0.12927	134.1	134.7	146
21	57N73(m)s	1121	12.68	0.00054	0.05574	0.34207	83.7	83.9	91
	(sp)s	297	3.18	0.01410	0.25517	1.21780	83.3	84.1	109
22	KC13(c)s	850	9.77	0.00021	0.05102	0.19486	85.1	85.4	93
	(m)s	988	11.49	0.00018	0.05037	0.19390	86.1	86.2	89
23	KC20(m)s	969	11.15	0.00027	0.05181	0.19220	85.1	85.5	93
24	OW4(c)s	260	3.54	0.00112	0.06549	0.30563	100.5	102.3	148
	(m)s	306	4.26	0.00106	0.06374	0.45600	102.8	103.0	108
25	OW34(m)s	383	5.31	0.00064	0.05774	0.18730	102.5	102.8	112
26	OW6(m)s	1007	22.50	0.00018	0.05227	0.20414	164.4	165.1	176
	(f-1)s	1155	25.95	0.00017	0.05195	0.20861	165.2	165.5	171
	(f-2)s	1152	---	---	---	---	166.1	166.4	171
	(sp)s	170	3.65	0.00901	0.18139	1.22920	158.3	158.6	164
27	OW7(n)s	1498	22.75	0.00131	0.06741	0.23915	112.2	112.1	111
28	OW19(m)s	1140	25.23	0.00066	0.05924	0.23965	162.9	163.4	172
29	E27-9(m)t	777	16.06	0.00047	0.05750	0.28337	152.1	156.2	219
	(f)t	825	16.94	0.00051	0.05685	0.27140	151.0	151.9	165
30	W24(c)t	422	6.33	0.00077	0.06054	0.20612	110.6	112.6	156
	(m)t	645	9.01	0.00043	0.05506	0.20136	103.2	104.6	138
31	W26(c)t	202	3.12	0.00136	0.06847	0.17683	114.5	114.8	123
32	W16(m)t	135	2.11	0.00079	0.06321	0.16195	115.6	123.2	271
	(f)t	204	3.12	0.00073	0.05966	0.15040	113.1	114.6	147
33	W18(c)t	362	4.94	0.00032	0.05312	0.10331	100.9	101.8	123
	(m)t	411	5.86	0.00040	0.05629	0.10429	105.3	110.1	214
34	W19(m)t	955	13.11	0.00013	0.05076	0.10002	101.4	102.9	139
	(f)t	988	12.92	0.00012	0.05041	0.10073	96.6	98.0	130
35	SQ57(m)s	977	13.18	0.00088	0.06150	0.26400	99.8	100.2	110
	(f)s	923	12.30	0.00071	0.05831	0.18350	98.4	98.3	97
36	SQ9(c)s	876	11.86	0.00047	0.05505	0.12685	100.1	100.2	104
	(m)s	1386	18.74	0.00086	0.06088	0.14590	100.0	100.6	116
37	SQ22(c)s	628	8.27	0.00035	0.05324	0.27375	97.3	97.6	104
	(m)s	664	8.74	0.00027	0.05220	0.15864	97.3	97.9	113
38	SQ75(m)s	993	13.48	0.00013	0.05042	0.13807	100.4	101.2	122
	(f)s	1158	15.75	0.00046	0.05505	0.21969	100.6	100.9	110
39	SQ7(f)s	928	12.84	0.00042	0.05417	0.23300	102.3	102.2	100

TABLE 1. (continued)

Sample	Field	Concentration, ppm		Isotopic Composition			Age, m.y.		
		^{238}U	$^{206}Pb^*$	$^{204}Pb/^{206}Pb$	$^{207}Pb/^{206}Pb$	$^{208}Pb/^{206}Pb$	$^{206}Pb^*/^{238}U$	$^{207}Pb^*/^{235}U$	$^{207}Pb^*/^{206}Pb^*$
40	SQ5(m)s	947	12.40	0.00027	0.05261	0.14220	96.8	98.2	131
	(f)s	1165	15.16	0.00020	0.05169	0.14440	96.2	97.8	136
41	SQ8(c)s	577	8.65	0.00038	0.05413	0.12365	110.7	111.3	125
	(m-1)s	704	10.94	0.00076	0.05983	0.13900	114.8	115.7	134
	(m-2)s	702	10.97	0.00024	0.05254	0.12213	115.4	116.8	146
	(m-3)s	726	11.14	0.00025	0.05241	0.12154	113.3	114.4	138
	(f)s	933	13.37	0.00011	0.05035	0.11772	105.9	107.3	138
	(sp)s	47.5	0.62	0.01719	0.30173	0.71404	96.1	96.0	95
42	SQ12(f)s	1560	21.72	0.00040	0.05482	0.15810	102.9	104.7	146
43	SQ48(m)s	1218	16.18	0.00013	0.05015	0.12024	98.2	98.6	108
	(sp)s	227	3.11	0.00618	0.13913	0.59288	101.2	101.6	111
44	SQ13(m)s	745	9.79	0.00063	0.05742	0.18095	97.1	97.5	107
	(m)s	963	12.78	0.00043	0.05471	0.19000	98.1	98.9	118
45	SQ46(m)c	1308	17.67	0.00055	0.05624	0.25590	99.3	99.5	105
	(c)s	1219	15.87	0.00010	0.04977	0.22355	96.3	96.9	116
	(sp)s	295	3.88	0.00557	0.12946	0.47530	97.7	97.0	80
46.	SQ61(c)s	4146	56.39	0.00055	0.05625	0.08818	100.5	100.8	107
	(m)s	4626	62.53	0.00040	0.05418	0.07422	99.9	100.5	115
47	SQ67(c)s	773	9.55	0.00045	0.05460	0.17788	91.5	91.6	95
	(m)s	858	10.52	0.00029	0.05231	0.18060	90.7	91.0	101
48	68M15(c)t	673	7.98	0.00062	0.05824	0.18976	87.9	90.2	151
	(m)t	673	8.04	0.00209	0.07973	0.24330	88.3	90.4	146
49	OW40(m)t	1064	11.98	0.00010	0.04927	0.17422	83.4	83.5	88
50	OW41(m-1)t	743	8.80	0.00060	0.05631	0.17866	87.6	87.1	74
	(m-2)t	828	9.67	0.00113	0.06436	0.30467	86.5	86.2	80
51	E27-3(f)t	1931	22.28	0.00129	0.06666	0.19000	85.4	85.3	83
	(m)t	1542	18.08	0.00090	0.06247	0.17457	86.8	89.2	155
52	W29(m-1)t	210	3.31	0.00109	0.06488	0.11527	116.3	117.4	141
	(m-2)t	191	3.07	0.00683	0.15253	0.37089	118.5	127.7	301
	(c)t	178	2.79	0.00125	0.06888	0.16871	116.0	120.9	218
53	W30(f)t	992	15.35	0.00011	0.05197	0.12068	114.2	118.6	209
	(m)t	657	9.92	0.00019	0.05421	0.13543	111.5	118.5	263
54	W31(m)t	380	5.51	0.00034	0.05512	0.16178	107.2	111.5	204
	(c)t	318	4.66	0.00019	0.05094	0.16232	108.1	107.9	103
55	W32(m)t	1064	14.91	0.00011	0.04992	0.07357	103.6	104.2	118
56	W34(m)t	1188	15.64	0.00015	0.05109	0.09212	97.3	99.0	139
	(f-1)t	1304	17.02	0.00035	0.05397	0.10247	96.4	98.0	136
	(f-2)t	1127	14.32	0.00019	0.05141	0.09578	94.0	95.3	130
57	SQ3(n)t	1034	13.80	0.00015	0.05115	0.09691	98.7	100.3	140
58	SQ15(f)t	808	10.87	0.00024	0.05260	0.11014	99.4	101.5	151
59	6-124(f-1)t	1338	15.04	0.00023	0.05238	0.21207	83.2	84.0	106
	(f-2)t	1454	18.60	0.00027	0.05227	0.20394	94.6	95.5	118
	(m)t	1035	12.81	0.00052	0.05693	0.19064	91.5	94.1	161
60	7-19(f)t	908	19.33	0.00013	0.05277	0.20516	156.5	161.6	237
	(m)t	748	16.27	0.00028	0.05610	0.22699	160.0	168.2	285
61	77-7(m)t	764	16.53	0.00078	0.06392	0.23200	159.2	169.1	310
	(f)t	974	19.54	0.00026	0.05435	0.23151	147.7	152.1	222
62	7-51(n)t	339	7.84	0.00024	0.05441	0.22280	169.9	174.2	233
63	8-38A(f)t	2946	61.31	0.00007	0.05123	0.13952	153.2	156.5	208
64	7-55(c)t	711	7.71	0.00330	0.09635	0.31428	80.2	80.3	84
	(f)t	624	6.82	0.00832	0.17027	0.48956	80.9	80.8	80
65	8-124-3(n)t	279	3.34	0.00699	0.15209	0.44038	88.3	90.2	142
66	8-54(m)t	764	15.87	0.00032	0.05401	0.16221	153.9	154.5	164
	(f)t	1590	33.59	0.00017	0.05218	0.11927	155.5	156.9	178
67	MA2(f-1)t	1408	41.64	0.00003	0.05135	0.12046	216.6	218.4	238
	(f-2)t	1498	42.98	0.00029	0.05499	0.12549	210.2	211.6	228
68	MA5(m)t	2817	77.4	0.00001	0.05124	0.06476	201.4	204.8	244
	(f)t	1607	40.14	0.00014	0.05243	0.08744	184.7	187.9	228
69	MA7(m)t	2615	55.55	0.00021	0.05401	0.21226	156.3	161.5	239
	(f)t	2414	40.10	0.00009	0.05167	0.25242	122.5	126.9	209
70	MA9(m)t	649	14.18	0.00019	0.05388	0.18215	160.7	166.2	245
	(c)t	540	11.68	0.00076	0.06224	0.19700	159.0	164.5	245

TABLE 1. (continued)

Sample	Field	Concentration, ppm		Isotopic Composition			Age, m.y.		
				^{204}Pb	^{207}Pb	^{208}Pb	$^{206}Pb^*$	$^{207}Pb^*$	$^{207}Pb^*$
		^{238}U	$^{206}Pb^*$	^{206}Pb	^{206}Pb	^{206}Pb	^{238}U	^{235}U	$^{206}Pb^*$
71	MA16(m)t	1113	31.91	0.00003	0.05101	0.11190	210.1	211.1	223
72	MA17(f)t	1644	45.16	0.00005	0.05127	0.09944	201.4	202.9	220
73	MA1(f)t	2092	43.89	0.00011	0.05252	0.10551	154.4	159.3	234
74	OW2(f)t	1934	52.03	0.00011	0.05227	0.10743	197.3	199.6	227
75	MG6-24(m)s	315.7	6.73	0.00054	0.05778	0.15114	157.0	158.8	186
76	F1-57(c)s	491	11.69	0.00068	0.05936	0.22890	175.1	174.4	164
77	02-26(c)s	468	11.14	0.00173	0.07499	0.24590	174.9	175.1	178
78	COSO-1(m)s	628	13.27	0.00223	0.08154	0.32015	155.9	156.1	161
	(c)s	642	13.70	0.00274	0.08990	0.33576	157.1	158.5	180
79	GRB(f)s	514	12.97	0.00289	0.09210	0.38847	185.1	185.2	186
	(m)s	420	10.68	0.00377	0.10503	0.42542	186.7	186.8	189
80	JMP(f)s	914	19.99	0.00060	0.05757	0.20680	160.9	159.7	143
	(m)s	801	17.55	0.00040	0.05512	0.22270	161.2	161.1	160
81	OW11(m)s	423	8.85	0.00088	0.06211	0.28088	153.9	154.1	156
	(f)s	670	14.00	0.00063	0.05836	0.28554	153.7	153.7	154
82	OW37(c)t	243	4.84	0.00149	0.07067	0.24139	146.9	146.4	139

Zircon: c, coarse (>200 mesh); m, medium (<200 mesh, >325 mesh); f, fine (<325 mesh); n, unsieved. Sphene: sp, (all >200 mesh). t, spiked with ^{205}Pb-^{235}U and s, spiked with ^{208}Pb-^{235}U. Isotopic ratios corrected for mass fractionation of 0.1 ± 0.03% per mass unit on basis of replicate analyses of U.S. National Bureau of Standards Pb standards SRM 981, 982, and 983. Constants used in age calculation: $\lambda^{238}U = 1.5513 \times 10^{-10}$, $\lambda^{235}U = 9.848 \times 10$ [Jaffey et. al., 1971]; $^{238}U/^{235}U = 137.88$.

*Indicates radiogenic Pb, corrected for common Pb by using isotopic composition of Pb from feldspars or whole rocks or lab blanks ($^{206}Pb/^{204}Pb$ = 18.5-19.4; $^{207}Pb/^{204}Pb$ = 15.60-15.65).

Table 2. Summary of preferred intrusive ages

Locality no.	Pluton	Preferred Age m.y.	Age Type	Age Group[3]
1	unnamed	114	IC	EK
2	unnamed	112	IC	EK
3	unnamed	111	IC	EK
4	gabbro	(<100)	I	LK
5	unnamed	(>145)	D	J
6	unnamed	111	IC	EK
7	unnamed	112	IC	EK
8	unnamed	106	IC	EK
9	unnamed	128	IC	EK
10-11	Yucca Point	110	IC, ED(2.5)	EK
12	Brush Canyon (Dike)	86	IC	LK
13-14	Tombstone Creek	99	IC, I	LK
15	Lightning Creek	108	IC	EK
16-17	Lookout Creek	97	IC, ED(6.3)	LK
18	North Dome	89(?)	IC	LK
19-20	North Mountain	(>134) or (≤89)	D or I	EK
21,22,23	Paradise	83-86	IC, ED(1.0)	LK
24	Bullfrog	103	IC, ED(2.3)	EK
25	Dragon	103	IC	EK
26	Woods Lake mass, Tinemaha granodiorite	165	IC, ED(1.7)	J
27	Independence	112	IC	EK
28	Santa Rita Flat	163	IC	J
29	Paiute Monument	(<152)	I	J
30	unnamed	(>111)	D	EK
31	unnamed	115	IC	EK

TABLE 2. (continued)

Locality no.	Pluton	Preferred Age m.y.	Age Type	Age Group[3]
32	unnamed	(<113)	I	EK
33	unnamed	(<101)	I	EK
34	unnamed	(<97)	I	LK
35-39	Giant Forest	97 - 102	IC, ED(1.4), EC	LK
40	Giant Forest( )	(>97)	D	LK
41	Lodgepole	(>115)		EK
42-43	Big Meadow	98	IC, I	LK
44-45	Weaver Lake	97-99	IC, ED(3.0)	LK
46	alaskite	100	IC, EC	LK
47	Mitchell Peak	91	IC, ED(0.8)	LK
48	Sugarloaf	(<88)	I	LK
49	Whitney	83	IC	LK
50	Lone Pine	87	IC, ED(1.1)	LK
51	Alabama Hills	85	IC, I	LK
52	unnamed	(116)	I	LK
53	unnamed	(<112)	I	LK
54	unnamed	108	IC, I	LK
55	unnamed	104	IC	LK
56	unnamed	(>97)	D	LK
57	Cactus Point	(<99)	I	LK
58	Potwisha	(<99)	I	LK
59	unnamed	(>95)	D	LK
60	unnamed	(>160)	D	J
61	unnamed	(>159)	D	J
62	unnamed	(>170)	D	J
63	Red Mountain Creek	(>153)	D	J
64	dike	80	IC, ED(0.7)	LK
65	dike	(<88)	I	LK
66	White Fork	(156)	D	J
67	Benton Range	(>217)	D	T
68	Benton Range	(>201)	D	T
69	dike	(148)	D+I	J
70	Benton Range	(>161)	D	T
71	dike	210	IC	T
72	Lee Vining Canyon	(210)	D	T
73	Lee Vining Canyon	(210)	D	T
74	Tunsten Hills	(210)	D	T
75	granite of Goddard Pendant	(>157)	D	J
76	Long John	175	IC	J
77	Darwin	175	IC	J
78	Coso	156	IC, ED(1.2)	J
79	Bendire Canyon	185	IC, ED(1.6)	J
80	Maturango	160	IC, EC	J
81	S. Argus Range	154	IC, EC	J
82	E. Spangler Hills	147	IC	J

Numbers in parentheses are discordant U-Pb ages; ranges of ages indicate possible cooling time. Models used to interpret the U-Pb ages: IC, internal concordant; EC, external concordant; ED, external discordant (age differences in m.y.); I, inherited or entrained old zircons; D, thermal disturbance. LK, Late Cretaceous (80-100 m.y.); EK, Early Cretaceous (100-140 m.y.); J, Jurassic (140-195 m.y.); T, Triassic (195-225 m.y.).

$^{207}Pb/^{206}Pb$ ages. Since the sphene $^{206}Pb/^{204}/Pb$ and $^{207}Pb/^{204}Pb$ ratios are less radiogenic (ranging from 60 to 180 and 18 to 23, respectively), the uncertainty in calculating radiogenic Pb, especially ^{207}Pb becomes significant. For example, analytical errors in the calculated $^{206}Pb/^{238}U$ and $^{207}Pb/^{235}U$ ages for a sphene from the North Dome pluton (sample 18) are 1.2 m.y. and 6.1 m.y., respectively.

To determine the reproducibility of the analytical results, a few samples and standards have been measured in duplicate. The isotopic results of four Pb standards (NBS SRM 981, 982, 983, and CIT Pb Standard) shown in Table 3 indicate that (1) all measured $^{207}Pb/^{206}Pb$ ratios agree within 0.1% with the nominal values, and (2) the value of $^{204}Pb/^{206}Pb$ measured ranges from 0.06 to 0.00037 and also agrees within 0.2% to 0.5% with the nominal values. The results of two U standards (NBS SRM U500 and U050) shown in Table 4 give the values of the mass fractionation factors, 0.09% ± 0.2% and 0.044 ± 0.2% per mass unit,

TABLE 3. Lead Isotopic Standards

Standards		Isotopic Composition		Age, m.y.
		$^{204}Pb/^{206}Pb$	$^{207}Pb/^{206}Pb$	$^{204}Pb/^{206}Pb$
NBS SRM 98*		0.059042 (37)	0.91463 (33)	2.1681 (8)
This work	M	0.059085 (30)	0.91420 (30)	2.1631 (6)
	N	0.05895	0.9152	2.1681
NBS SRM 982*		0.027219 (27)	0.46707 (20)	1.00016 (36)
This work	M	0.027231 (55)	0.46661 (40)	0.99825 (40)
	N	0.02718	0.4670	1.00016
NBS SRM 983*		0.000371 (20)	0.071201 (40)	0.013619 (24)
This work	M	0.000369 (8)**	0.071188 (70)	0.013624 (40)
	N	0.000369	0.07117	0.013619
C.I.T. Pb Std		0.060151 (63)	0.93081 (35)	2.1835 (10)
This work	M	0.060200 (50)	0.92991 (30)	2.1775 (8)
	N	0.06003	0.9312	2.1835

Amount of Pb measured per analysis is about 100 ng. Numbers in parentheses are 2σ errors of the last significant figures; values from this work are average of six analyses. M, measured values; N, normalized values.

*From Catanzaro et al. (1968).

**Measured with an electron multiplier; all other ratios are measured with a Faraday cup collector.

respectively, for different ranges of the $^{235}U/^{238}U$ ratio. A value of 0.1 ± 0.2% per mass unit was used for correction.

One zircon fraction of the following samples was analyzed in duplicate to determine the reproducibility of the $^{206}Pb/^{238}U$ results: (1) sample 11 shows good agreement, (2) sample 26 also shows good agreement in the concentration of U, (3) sample 41 shows 1.9% variation, (4) sample 50 shows 1.3% variation, (5) sample 52 shows 1.9% variation, (6) sample 56 shows 2.5% variation, (7) sample 59 is highly discordant, and (8) sample 67 shows 3% variation. It is apparent that some samples show more variations in $^{206}Pb/^{238}U$ ages in duplicate analyses than the error expected from the analytical technique. Some of these samples are clearly discordant because analyses of different size fraction of the same samples are also discordant.

TABLE 4. Uranium Isotopic Standards

Standards	$^{235}U/^{238}U^2$
NBS SRM U500*	0.9997 (9)
This work	1.0024 (10)
NBS SRM U050*	0.05278 (5)
This work	0.05285 (5)

Amount of U measured per analysis is about 500 ng. Atomic ratios; numbers in parentheses are 2σ errors of the last significant figures.

*From Catanzaro et al. [1968].

External Concordancy

The differences in the $^{206}Pb/^{238}U$ ages between different size fractions of zircons or between zircon and sphene from the same rocks are plotted against that of the coarsest zircon in Figure 4. Only about 50% of the zircons and two out of seven sphene U-Pb ages agree within ±1 m.y., the rest are clearly discordant. These discordant samples may indicate disturbances in the U-Pb systems by geological processes or sample heterogeneity or other processes.

Interpretation of Discordant U-Pb Ages

The U-Pb ages determined on zircon are commonly discordant. If certain rather general conditions generate a systematic relation between the coupled ^{206}Pb-^{238}U and ^{207}Pb-^{235}U systems, it is possible to determine the primary age of a sample even when the U-Pb systems are open. Since the parents (^{238}U and ^{235}U) and daughters (^{206}Pb and ^{207}Pb) are isotopes of given elements, they will not fractionate during geochemical processes and will produce regular and predictable behavior on a concordia diagram [Wetherill, 1956].

Several possibilities can generate a linear relation in the U-Pb concordia diagram. The following are some of the more general possibilities.

U-Pb Disturbance

Pb-loss model. Generally, refractory minerals such as zircon lose only a fraction of their radiogenic Pb, and zircon crystals in an igneous rock may lose varying fractions of their radiogenic Pb. In such a case, a straight line fitted to data points (e.g., A, B, and C, Figure 5) for these cogenetic zircons will intersect

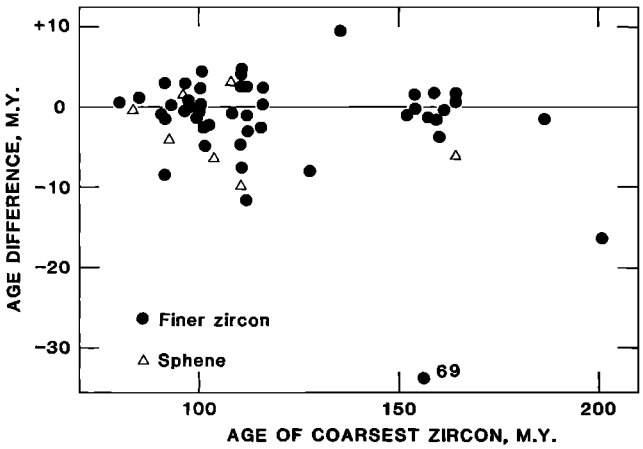

Fig. 4. Difference of $^{206}Pb^*/^{238}U$ ages of sphene and finer grained zircon as compared with that of the coarsest zircon in the same rock sample.

the concordia at two points. The upper intersect represents the primary age (T_1), and the lower intersect represents the time of the episodic event (T_2).

U-gain model. In the previous model, zircon crystals which suffer Pb loss as a result of thermal metamorphism, or chemical weathering, may gain U by metamorphic overgrowth. Other U-bearing minerals such as sphene may be formed during the metamorphism. The observed data array for the U-gain model is similar to that for the Pb-loss model, although the mechanism for parent-daughter transports are different. These data show a 'normal' sequence of discordancy (i.e., $^{206}Pb/^{238}U<^{207}Pb/^{235}U<^{207}Pb/^{206}Pb$ age).

Pb-gain or U-loss model. If a sample with age T_1 gains radiogenic Pb or loses U during an episodic event at time T_2, it plots above the concordia curve (e.g., D, Figure 5). In this case it shows a reversed sequence of discordancy (i.e., $^{207}Pb/^{206}Pb<^{207}Pb/^{235}U<^{206}Pb/^{238}U$ age). In practice, if there exists certain analytical problems such as (1) incomplete sample dissolution or (2) incomplete mixing of the U-Pb tracer with the sample fluoride solution (in particular, U isotopes) in analyzing a zircon sample of age T_1, the result (e.g., D', Figure 5) plots above the concordia curve and along a chord connecting the origin and T_1.

Sample heterogeneity

Although zircons easily lose some of their radiogenic Pb, some zircons may survive the magmatic condition and possibly retain some of their radiogenic Pb.

Inherited zircons. Partial melting of a source rock of age T_1 generates a granitic magma. The granitic magma was emplaced and forms a pluton at time T_2. Zircons in the granitic rock on the whole are newly formed crystals, and yield concordant U-Pb ages of T_2. If a small part of the zircons in the original source rock survives the partial melting event and is present in the granitic rock as xenocrysts (or as the core of some newly formed crystals), the zircon mixture from the granitic rock will show discordant ages. In this case, the data array will plot along a chord connecting T_1 and T_2, but plot close to the lower intersect (T_2). If the source rocks contain detrital zircons of different ages, the resulting data plot in a field (e.g. Z, Figure 5) close to T_2.

Entrained zircon. During the ascent and emplacement of a granitic magma, it could also entrain zircons of very different ages by processes such as crustal anatexis and assimilation of country rocks. The resulting data array is similar to the previous case (inherited zircon), but the meaning of the 'source' age T_1 is very different.

U-Series Disequilibrium and Recoil Loss

The previous discussions are based on the assumption that U isotopes are in secular equilibrium with their intermediate daughter isotopes (IDI), and each U atom decays to form one Pb atom. Since U does not decay directly to Pb, if the IDI are not present in equilibrium amounts, the normal equation (1) will not be valid. In the study of the Tertiary Tatoosh complex, Mattinson [1973, 1977] found that the $^{207}Pb/^{206}Pb$ ratios in some very young zircons are much too high (~2%) for their $^{206}Pb/^{238}U$ ages. He interpreted these anomalous $^{207}Pb/^{206}Pb$ ratios as modified by incorporation of IDI (^{230}Th and ^{231}Pa) in nonequilibrium amounts during crystallization or preferential losses of IDI (in particular, ^{222}Rn and ^{219}Rn) during cooling. The effects of U-series disequilibrium should be negligible for most samples (80-210 m.y.) analyzed in this work [Mattinson, 1973]. Recoil losses of IDI from the U series subsequent to crystallization are possible and may be common if the samples were under high-temperature conditions for a long time. Some IDI such as Rn

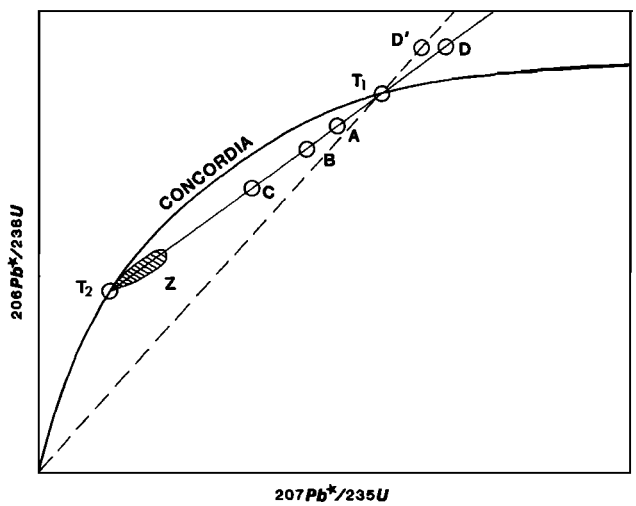

Fig. 5. $^{206}Pb^*/^{238}U$ versus $^{207}Pb^*/^{235}U$ diagram showing concordia curve and examples of hypothetical data points according to models for the interpretation of discordant U-Pb ages discussed in the text.

may escape more easily than others, and the extent of losses may vary between samples, resulting in different cooling ages. The small variations in the U-Pb ages from the Giant Forest-alaskite (GFA) sequence (next section) may indicate different cooling times among various parts of the plutonic complex. In general, for samples as old as those from the Sierra Nevada batholith, the effects of U-series disequilibrium or recoil losses of IDI may be small and could be masked by other mechanisms of disturbance or sample heterogeneity.

The above discussions indicate that the graphic presentation of discordant U-Pb ages for samples which have experienced an episodic event or have heterogeneous zircon populations is similar, but the meaning of ages T_1 and T_2 are quite different. It is therefore difficult to interpret discordant U-Pb ages on the basis of only one zircon analysis.

The 133 zircon and 7 sphene separates indicate that some of the samples may have experienced U-Pb disturbances, and some may have heterogeneous zircon populations. For those discordant samples, the U-Pb data were plotted and evaluated on the concordia diagram. However, since the concordia curve between the origin and 220 m.y. is close to a straight line, it is often difficult to fit a chord to the data array. In addition, the low enrichment of radiogenic ^{207}Pb relative to ^{206}Pb in most samples makes the $^{207}Pb/^{206}Pb$ (~0.05) more difficult to measure precisely. Therefore, the $^{206}Pb/^{238}U$ age is considered the more precisely determined age.

In some samples, although the individual analyses show concordant U-Pb ages, different zircon size fractions show more variation in the $^{206}Pb/^{238}U$ age than that estimated from analytical uncertainties (0.6 m.y.). Apparently some other factors such as the effects of U-series disequilibrium (<0.5 m.y.), possible differences in recoil loss of intermediate isotopes during initial cooling, or analytical problems also affect the 'accuracy' of the U-Pb ages. Considering the above factors and judging from the reproducibility of duplicate analyses on some Cretaceous samples (11, 26, 41, 50, and 52), these zircon ages will be inferred to represent emplacement ages if they are concordant to 2% (Table 2).

A detailed evaluation and interpretation of each discordant U-Pb age will be given in the following appropriate section. Based on this interpretation, an optimum age can be estimated for each pluton which is considered a good approximation of the emplacement age of the pluton (Table 2). In addition, the following criteria are considered for estimating the preferred age: (1) intrusive relations where data are available, (2) U-Pb ages determined on different size fractions or different samples of the pluton, (3) U-Pb ages from both zircon and sphene, and (4) U-Pb ages and hornblende K-Ar ages from the same pluton.

Nested Plutons

Four plutons ranging in composition from granodiorite to alaskite were emplaced into a total area of at least 340 km^2 in Sequoia National Park (Figure 2). The sequence of plutons, listed from old to young, includes the Giant Forest, Big Meadow, Weaver Lake, and alaskite [Ross, 1958], and shows a nested zonal pattern with the older and more mafic members on the border and the younger and more silicic ones in the central area. Field and petrographic studies [Ross, 1958] indicate that the sequence of plutons is genetically related and that their compositions define a uniform differentiation trend. A total of 11 samples (samples 35 to 40, 42 to 46) were collected from the Giant Forest-Alaskite sequence (GFA sequence), and 19 zircon and 2 sphene separates have been analyzed for U-Pb ages. The results are shown in Table 1 and are plotted in Figure 6 on a concordia diagram.

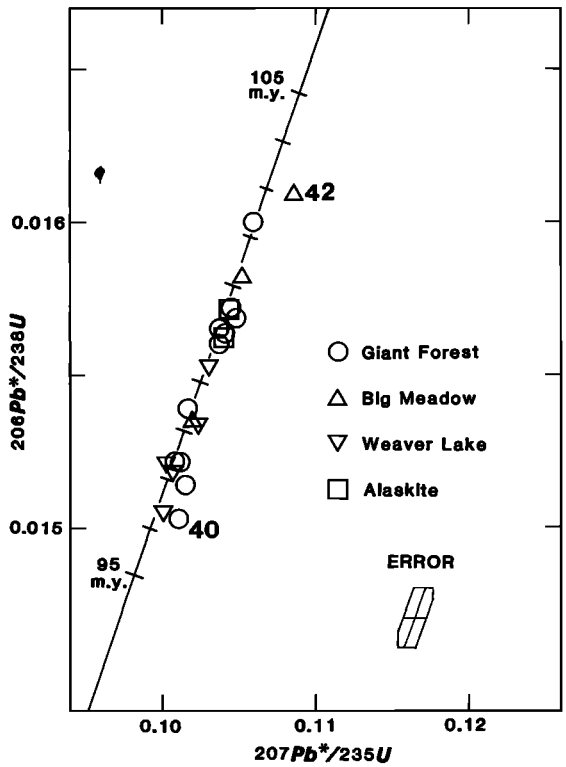

Fig. 6. $^{206}Pb^*/^{238}U$ versus $^{207}Pb^*/^{235}U$ diagram for zircon and sphene data from the Giant Forest- Alaskite sequence in the central Sierra Nevada batholith.

The zircon U-Pb data from the GFA sequence have the following characteristics:

1. The $^{206}Pb/^{238}U$ and the $^{207}Pb/^{235}U$ ages are concordant within ±0.6 m.y. for most individual analysis (15 out of 21).

2. The $^{206}Pb/^{238}U$ ages for all the 'concordant' samples show a limited range (96.3-100.6 m.y.).

3. A few data points (samples 42 and 40) are discordant and plot below the concordia curve.

4. The U-Pb ages of most fine-grained zircon fractions (which have relatively high U concentrations) are identical to that of the corresponding coarser (and lower U) fractions.

5. Data from different members of the sequence do not show large age differences

indicating a relative short period of emplacement of the whole sequence. The spread of data points in Figure 6 corresponding to a value of 99 ± 3 m.y. has about 5 times the dispersion expected from analytical error (±0.6 m.y.). In addition, analyses of different size fractions of zircons from the same rock show from good agreement (sample 37) to large variation (3 m.y., sample 45) in the $^{206}Pb/^{238}U$ age, although the individual analysis has concordant $^{206}Pb/^{238}U$ and $^{207}Pb/^{235}U$ ages (±0.6 m.y.). This discrepancy may result from geological processes such as the mobility of U and Pb after the crystallization of the samples or the presence of 'inherited' zircon or differential cooling.

In a series of samples collected from the margins to the core of the plutonic complex, the $^{238}U-^{206}Pb$ ages decrease regularly from 102 m.y. to 97 m.y. Similar trends were also observed between samples 36 and 44 or 46 and 43. These data suggest that the differences in U-Pb ages may represent different cooling times between the margin and center of a plutonic complex. The younger age of 97.3 m.y. (sample 37) from an aplite dike in the Giant Forest pluton indicate that magmatic intrusion was still active after initial emplacement and crystallization of the major sequence took place. Some of the discordant U-Pb ages clearly could not result from differential cooling. Since the concordia curve between the origin and 110 m.y. is essentially a straight line (Figure 6), it is difficult to resolve discordance patterns using this diagram. One of the most discordant samples (42) plots below the concordia curve toward the older side (Figure 6), indicating the possible presence of 'inherited' (or entrained) zircon. If the emplacement age of the GFA sequence is ~99 m.y., the age of the source of the 'inherited' (or entrained) zircon in sample 42 is estimated at 1 b.y. A similar study of the 'inherited' zircon problem was reported by Mattinson [1978] for granitic rocks about 104 m.y. old from the Salinian block of western California.

Sample 40 is from a granoitoid body separated from the main GFA sequence by a roof pendant (Figure 2). Although interpreted as part of the Giant Forest pluton [Ross, 1958], it could be a separate unit. Somewhat younger (96 m.y.) and discordant ages are also observed in the nearby sample 56.

In summary, the entire GFA sequence was probably emplaced in a relatively short period of time (1 to 2 m.y.). Cooling of the plutonic complex took place from the margin toward the center in about 3 m.y. while late-stage magmatic intrusion was still active.

Mafic Inclusions

Mafic inclusions are abundant in the Sierra Nevada granitoids [Pabst, 1936; Bateman et al., 1963; Moore, 1963]. A number of hypotheses have been considered to explain the origin of the mafic inclusions: (1) the inclusions are fragments of partly assimilated country rocks, (2) they are fragments of an earlier crystallized mafic phase of the intrusive mass, (3) they are refractory residues left over from the partial melting of source material, (4) they are aggregates of early formed minerals, or (5) they represent mafic magma which was entrained within and chilled by the more silicic host. The single mafic inclusion sample investigated here (sample 35) is about 30 cm in greatest dimension and was collected from the Giant Forest pluton about 5.6 km away from the nearest roof pendant rocks. It contains abundant plagioclase, hornblende, and biotite with accessory zircon, sphene, and apatite. K-feldspar and quartz are minor relative to the host rock. Two fractions of zircon from the inclusion yield U-Pb ages of 97 and 100 m.y., respectively, which fall within the range of ages of the GFA sequence (99 ± 3 m.y.). The zircon U-Pb ages do not indicate inherited zircon, and both Pb and Sr isotopes [J. H. Chen and G. R. Tilton, unpublished data, 1982) show similar initial ratios for the mafic inclusion and the host granitic rocks. These results, plus field and petrographic studies, suggest that (1) both the mafic inclusion and the granodiorite host rock were derived from a common source, or (2) the mafic inclusion was totally equilibrated with the granodioritic magma. The first model would satisfy hypothesis 2 and 4 for the origin of the mafic inclusions, while the second model satisfies all five hypotheses. The problem concerning the origin of mafic inclusions definitely requires further investigations than this preliminary study, possibly in areas where inclusions are large enough and where the cooling rate is fast enough to preserve possible original isotopic differences.

Age of Granitoids in the Sierra Nevada

Most samples analyzed in this report are from a belt between latitude 36° and 37°N. in the central Sierra Nevada batholith (Figure 2). Additional samples were collected from eastern California between the Garlock fault and latitude 38°N. (Figure 3). Collection of some samples, especially the Triassic ones in the Lee Vining area, was guided by the work of Evernden and Kistler [1970]. The following discussion will focus on the U-Pb ages determined from this work but will include results from Stern et al. [1981] on granitoids between latitude 37° and 38°N. and also from Saleeby and Sharp [1980] on rocks from the western Sierra Nevada foothills. The intrusive ages of granitic plutons will be discussed in the following groups: Triassic, Jurassic, Early Cretaceous, and Late Cretaceous (time scale follows that of Van Eysinga 1975]. The available data permit age estimates for the ~25,000 km^2 of Mesozoic granitic plutons in the area of Figure 3.

Triassic (195-225 m.y.)

Triassic granitic plutons in the study area occur in the Lee Vining-Bishop area in the east-central Sierra Nevada-White Mountains region (Figure 3). About 520 km^2 of Triassic granitic rocks (2%) are exposed in the area of Figure 3. Five samples (67, 68, 71, 72, and 74) indicate a Triassic age. Following Stern et al. [1981], these rocks probably belong to the

Scheelite sequence which represents one of the oldest intrusive events in the Sierra Nevada region. The rocks of the Scheelite sequence crop out discontinuously through Cenozoic deposits, and much larger areas are probably present. Two analyses of a granodiorite of the Benton Range (sample 67) from east of Lee Vining yield slightly discordant $^{206}Pb/^{238}U$ ages of 217 and 210 m.y. These U-Pb ages are comparable with the 214 m.y. reported by Stern et al. [1981] from the same area. Granitic and mafic dikes cut the quartz monzonite of Lee Vining Canyon in the eastern Sierra Nevada about 25 km southwest of sample 67. A sample of a granitic dike (sample 71) yields concordant U-Pb ages of 210 m.y. Both the host rock and the dike have $^{207}Pb/^{206}Pb$ ages about 220 m.y. The younger $^{206}Pb/^{238}U$ age (201 m.y.) of the host rock may indicate disturbance by later intrusions. Quartz monzonite of Lee Vining Canyon on the Tioga Road (sample 73) yields discordant U-Pb ages with a $^{206}Pb/^{238}U$ age of 154 m.y. This sample is from about 10 km west of Lee Vining, close to a locality where Evernden and Kistler [1970] reported a hornblende K-Ar age of 211 m.y. (this and all K-Ar ages are adjusted to new decay constants [Steger and Jager, 1977]. Results for sample 73, together with data from several other samples from this area are shown on the concordia diagram of Figure 7. The $^{207}Pb/^{206}Pb$ ages of all these samples (67 to 74) from the Lee Vining area range from 209 to 245 m.y. The maximum K-Ar age of the granodiorite of the Benton Range is 215 m.y. [Evernden and Kistler, 1970]. The emplacement age of the Scheelite sequence is probably about 210 m.y., based on the granitic dike ages (sample 71), which are close to the maximum K-Ar age. The total time span for the emplacement of the Scheelite sequence could not be estimated on the basis of available data so far. The slightly older $^{207}Pb/^{206}Pb$ ages of some of the samples might indicate the presence of 'inherited' or entrained old zircon, although no distinctive 'older' zircon cores were observed or analyzed. If the emplacement age of the quartz monzonite of Lee Vining Canyon (sample 73) is also about 210 m.y. (suggested by Rb-Sr whole rock dating [Kistler, 1966b, and unpublished data, 1981]), then the observed discordant U-Pb data could be explained by the disturbance model (Pb loss or U gain) and probably were caused by the intrusion of Late Cretaceous plutons to the west.

Another specimen of the granodiorite of the Benton Range (sample 68) from 45 km east-southeast of Lee Vining yields discordant zircon U-Pb ages with $^{206}Pb/^{238}U$ age of 201 and 185 m.y., respectively. Evernden and Kistler [1970] reported a hornblende K-Ar age of 215 m.y. and a biotite K-Ar age of 211 m.y. for a sample from this locality. The U-Pb result of this sample 68 might also indicate the effect of disturbance (Figure 7). A sample 74 of the Tungsten Hills quartz monzonite yields discordant U-Pb ages with a $^{206}Pb/^{238}U$ age of 197 m.y. Stern et al. [1981] report a $^{208}Pb/^{238}U$ age of 202 m.y. which is within 2% of the result of this work, on samples from the same pluton.

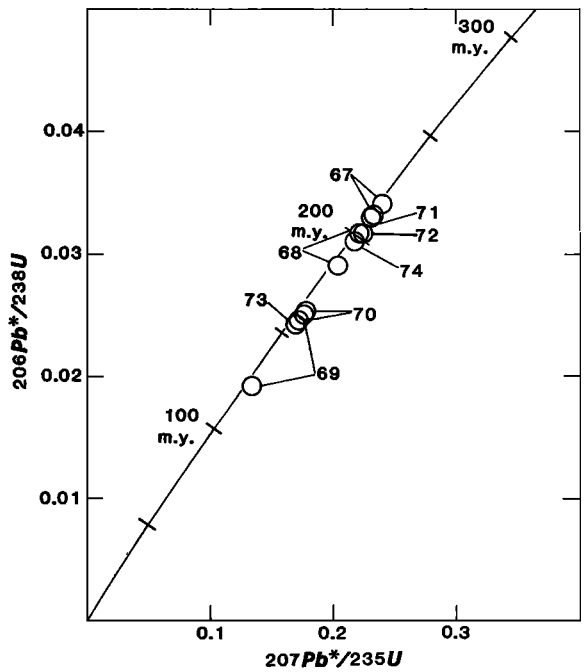

Fig. 7. $^{206}Pb^*/^{238}U$ versus $^{207}Pb^*/^{235}U$ diagram for zircon data from Jurassic and Triassic granitic rocks.

Available age data from the Lee Vining-Bishop area clearly indicate the existence of Triassic intrusions emplaced about 210 m.y. ago. According to Evernden and Kistler [1970, plate 2] and Stern et al. [1981] these intrusions underlie an area of at least 2500 km , extending from the latitude of Bishop northward beyond the limits of the map area (Figure 3).

Jurassic (140-195 m.y.)

Plutons which give Jurassic K-Ar and U-Pb ages occur most commonly on the eastern side of the Sierra Nevada batholith, in the Inyo-White Mountains, and Argus Range (Figure 3). Some remnants of Jurassic rocks are present within the Cretaceous plutons in the central Sierra Nevada. A few Jurassic plutons are also present in the Western Metamorphic belt in the Sierra Nevada foothills. Jurassic plutons crop out over 3800 km^2 of the area of Figure 3 (15% of the area of Mesozoic granitic rocks).

About 50 km southeast of Lee Vining, a prominent swarm of rhyolite-granite porphyry dikes intrude metamorphic rock and the granodiorite of the Benton Range [Rinehart and Ross, 1957]. Analyses of a dike in this swarm (sample 69) yielded very discordant U-Pb ages (Figure 4), with $^{206}Pb/^{238}U$ ages of 123 m.y. (fine zircon) and 156 m.y. (medium zircon). The U-Pb ages of the host rock (sample 70) are also discordant with a $^{206}Pb/^{238}U$ age of 159-161 m.y. The $^{207}Pb/^{206}Pb$ age of both rocks range from 209 to 245 m.y. The U-Pb data of these samples can be explained by the disturbance model. Probably, the host rock is as old as 245 m.y., and the dikes represent a northern extension of the Independence dike

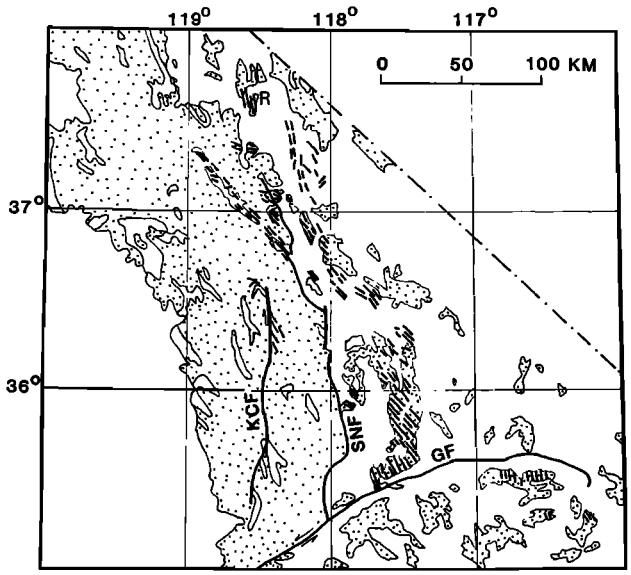

Fig. 8. Late Jurassic Independence dike swarm of eastern California after Moore and Hopson (1961), Chen and Moore (1979), and Smith (1962). Rhyolite porphyry dikes (R) of Rinehart and Ross (1957) are tentatively assigned to the swarm. Symbols: KCF, Kern Canyon fault; SNF, Sierra Nevada frontal fault; GF, Garlock fault.

swarm (Figure 8) dated to the south at 148 m.y. [Chen and Moore, 1979]. Such a correlation is clearly tentative and further age data are required to date satisfactorily this important dike swarm. The higher $^{207}Pb/^{206}Pb$ ages for the dike sample (sample 69) could be due to zircon entrained from the granodiorite. Both the host rock and the dike may be disturbed by later thermal events.

Stern et al. [1981] report ages ranging from 155 to 172 m.y. for rocks of the Deep Springs sequence, the Palisade Crest sequence, and some separated unassigned plutons in the eastern Sierra Nevada-White Mountain area. Included are samples from two plutons in the Owens Valley area correlated with the Tinemaha granodiorite of the Palisade Crest sequence. Three of our analyses of sample 26 from the Woods Lake mass of the Tinemaha granodiorite 8 km west of Independence yield concordant U-Pb ages of 165 ± 1 m.y. Analyses of sample 28 from the Santa Rita Flat mass 15 km north-northeast of Independence are concordant at 163 m.y. Evernden and Kistler [1970] reported a hornblende K-Ar age of 159 m.y. on a sample from the Santa Rita Flat mass. The U-Pb ages from both the Woodlake and the Santa Rita Flat masses of the Tinemaha granodiorite show excellent agreement and are ~4 m.y. older than the K-Ar age. Samples from another mass of the Tinemaha granodiorite dated by Stern et al. [1981] are discordant with a $^{206}Pb/^{238}U$ age of 155 m.y. The K-Ar ages (hornblende) from the several other masses of Tinemaha granodiorite range from 170 to 183 m.y. [Kistler et al., 1965]. The discrepancy in ages could be due to correlation problems for the Tinemaha granodiorite.

South of the Santa Rita Flat pluton, quartz monzonite of the Paiute Monument pluton (sample 29) yields slightly discordant U-Pb ages, with a $^{206}Pb/^{238}U$ age of 152 m.y. Evernden and Kistler [1970] report two hornblende K-Ar ages of 167 m.y. from this pluton. Two granodiorite plutons (samples 63 and 66) from the eastern Sierra Nevada, west of Independence also yield slightly discordant ages with $^{206}Pb/^{238}U$ age of 153 and 156 m.y., respectively. Southeastward, two samples (samples 76 and 77) from small granitic bodies which were emplaced into Paleozoic sedimentary rocks yield concordant U-Pb ages of 175 m.y. Farther south, five samples (samples 78-82) from the Argus Range area give concordant U-Pb ages ranging from 147 to 187 m.y. Twenty kilometers east of Independence the Hunter Mountain batholith [Dunne et al., 1978], was emplaced about 174 m.y. ago (J. H. Chen, unpublished data, 1982).

Many of the Jurassic plutons (and some Triassic ones) are cut by dark dikes which probably belong to the Late Jurassic Independence dike swarm (Figure 8) [Moore and Hopson, 1961; Smith, 1962]. Chen and Moore [1979] obtained concordant U-Pb ages of 148 m.y. on the more silicic members of the dike swarm and older ages for plutons intruded by the dike swarm. Some sheared plutons are cut by dark dikes and are themselves enclosed by the Cretaceous plutons in the eastern Sierra Nevada. These plutons were probably once part of the Jurassic granitoid belt to the east but were fragmented and shouldered aside by the intrusion of younger Cretaceous plutons. An analysis of one such sheared granodiorite (sample 75) 40 km west of Bishop yields slightly discordant U-Pb ages, with a $^{206}Pb/^{238}U$ age of 157 m.y. Other plutons cut by abundant mafic dikes in this area are also assigned to the Jurassic Period (Figure 3). Three samples (60-62) from plutons cut by dark dikes and truncated and displaced by the Kern Canyon fault [Moore and du Bray, 1978] yield discordant U-Pb ages. The $^{206}Pb/^{238}U$ ages range from 148 to 170 m.y. The older $^{207}Pb/^{206}Pb$ ages (222 to 310 m.y.) of these samples suggest that their intrusive ages might be much older (Triassic).

Jurassic plutons are less abundant on the west side of the batholith in the area of Figure 3 and are generally found within or adjacent to the western Sierra Nevada metamorphic belt. A possible Jurassic intrusion (sample 5) south of Bald Mountain east of Fresno occurs in a migmatite zone. The sample yields discordant $^{206}Pb/^{238}U$ ages of 136 and 145 m.y. for two zircon analyses. Stern et al. [1981] suggest two Jurassic sequences, the Foothills sequence and the Jawbone sequence, and some unassigned plutons. Their U-Pb ages on these plutons are mostly discordant, with the $^{206}Pb/^{238}U$ ages ranging from 148 to 190 m.y. Saleeby and Sharp [1980] also report several Jurassic granitoids that intrude the Kings-River ophiolite belt (Triassic-Jurassic age [Saleeby, 1982]) in the southwestern Sierra Nevada foothills. Their U-Pb ages are mostly concordant within 2% and range from 144 to 170 m.y.

Cretaceous (65-140 m.y.)

The present distribution of plutons in the Sierra Nevada is dominated by granitic rocks of Cretaceous age. Within the area of Figure 3, Cretaceous plutons occupy 83% of the area of Mesozoic granitic plutons. With only a few exceptions, rocks of Early Cretaceous age lie to the west of rocks of Late Cretaceous age. The intrusions are generally younger eastward (Figure 3) and were emplaced during a continuous magmatic episode from 120 to 80 m.y.

Early Cretaceous (100-140 m.y.). Early Cretaceous plutons crop out over 7700 km^2; 36% of the granitic area of Figure 3 occupied by Cretaceous granitic rocks. Only two small dated plutons (<20 km^2) have zircon U-Pb ages between 128 and 135 m.y. The aplitic North Mountain 'hooded' pluton (samples 19 and 20) occurs 38 km west of Independence as a small pluton surrounded by a zone of biotite schist about 100 m thick and is not in direct contact with the surrounding granodioritic plutons [Moore, 1978]. Three zircon separates yield discordant U-Pb ages ranging from 123 to 135 m.y., although the individual separates are concordant to 0.6 m.y. The U-Pb data may be explained by the following model. The aplitic rock is a remnant of a pluton at least 134 m.y. old which was enclosed by younger intrusions. The younger U-Pb ages probably resulted by disturbance by the intrusion of the surrounding plutons. Since the ages (89 and 98 m.y.) of the surrounding plutons are not much younger than the age of the aplitic pluton, the displacement of the U-Pb data by disturbance will closely follow the concordia curve and yield nearly 'concordant' ages. Alternatively, the stock could originate by partial melting of an older source rock. Thus, the 'intrusive' age of the stock would be the lower intersect age on a concordia diagram (not shown) that is less than or equal to 89 m.y. Zircon from a quartz monzonite (sample 9) 66 km west of Independence yields concordant U-Pb ages of 128 m.y., which is also older than the surrounding rocks. The relation of this pluton to the adjacent plutons is not known.

Eleven samples (1-8, 10, 11 and 15) from a west-east traverse across about 55 km of the western Sierra Nevada batholith (Figure 2) give mostly concordant U-Pb ages of about 110 m.y. Some of these samples (4, 10 and 11) are discordant and might show the effects of either disturbance by the intrusion of Late Cretaceous plutons or by presence of inherited old zircon.

Several dated samples (30-33, 52-55) were collected in a second traverse about 40 km south. Samples from the south side of this traverse are from plutons which were emplaced into metamorphic rocks. Some of them (samples 52-54) have old $^{207}Pb/^{206}Pb$ ages ranging from 204 to 301 m.y., indicating the possible presence of inherited or more likely 'entrained' old zircon during the intrusion of the plutons. A granite of the Lodgepole pluton (sample 41) 58 km west of Lone Pine yields slightly discordant U-Pb ages with $^{206}Pb/^{238}U$ ages ranging from 106 to 115 m.y. An alaskite (sample 27) from the Independence pluton 7 km west of Independence yields concordant U-Pb ages of 112 m.y., although the specimen is partially weathered. Two other early Cretaceous plutons occur nearby east of the Sierra Crest. Both the Bullfrog pluton (sample 24) and the Dragon pluton (sample 25) yield concordant ages of 103 m.y. The Lightning Creek pluton (sample 15) 35 km west of Independence yields a concordant age of 108 m.y.

Saleeby and Sharp [1980] also reported several U-Pb ages ranging from 102 to 131 m.y. from granitoids which intruded into the Kings-Kaweah ophiolite belt. These rocks are in general more mafic than those discussed above and give older ages. Lower Cretaceous granitoids north of the traverse at the latitude of Fresno cover a large area. Stern et al. [1981] report several U-Pb ages from the Millerton sequence which range from 110 to 119 m.y. and from several isolated plutons which are about 110 m.y. old.

Late Cretaceous (80-100 m.y.). The remaining dated granitic rocks occur primarily in the eastern Sierra Nevada and are Late Cretaceous in age. They occur over 13,500 km^2 in Figure 3 and comprise the most voluminous age group including 53% of the area of Mesozoic granitic rocks. These granitoids form a continuous belt adjacent to, and east of, the early Cretaceous belt of the western Sierra Nevada. In the Kings Canyon area, granodiorite of the Tombstone Creek pluton (samples 13 and 14) and granodiorite of the Lookout Peak pluton (samples 16 and 17) intruded into the western and eastern borders of the Lightning Creek pluton (108 m.y. old, sample 15). Only one zircon fraction was analyzed for each sample from the Tombstone Creek pluton. One of the samples (14) was collected from west of the contact with a metavolcanic roof pendant and yields concordant U-Pb ages of 99 m.y. The other sample (13) was collected east of the contact with the metasiltstone unit of the Boyden Cave pendant and yields discordant U-Pb ages with a $^{206}Pb/^{238}U$ age of 116 m.y. Detrital zircons from the metasiltstone yield discordant U-Pb ages with a $^{206}Pb/^{238}U$ age of 542 m.y. and a $^{207}Pb/^{206}Pb$ age of 1.3 b.y. [Chen, 1977]. The older $^{206}Pb/^{238}U$ age from the second sample (sample 13) may indicate the presence of some entrained old zircons.

Analyses of zircons from one (17) of the samples from the Lookout Peak pluton yield concordant U-Pb ages of 97 m.y., and analyses of the other sample (16) yield discordant ages with a $^{206}Pb/^{238}U$ age of 104 m.y. The second analysis (sample 16) is slightly reversed-discordant and may have analytical problems. Results on sphene from this sample (16) give concordant U-Pb ages of 98 m.y. which agree with the first zircon analysis 17. The Giant Forest (sample 35-40), Big Meadow (samples 42-43), Weaver Lake (samples 44-45), and associated alaskite plutons (sample 46) occur about 55 km west of Independence, and all yield concordant ages of 99 ± 3 m.y. A small hand specimen from the North Dome pluton (sample 18) about 42 km west of Independence yields small amounts of zircon and sphene. U-Pb results on zircon are discordant with a $^{206}Pb/^{238}U$ age of 93 m.y., while results on sphene are concordant with U-Pb ages of 89 m.y. The sphene

U-Pb age (89 m.y.) of this sample is tentatively believed to be the emplacement age of this pluton. The granodiorite of Mitchell Peak pluton (91 m.y., sample 47) was emplaced east of the Giant Forest-alaskite sequence. The granodiorite of Sugarloaf pluton (88 m.y., sample 48) occurs east of the Mitchell Peak pluton. The large Paradise-Whitney sequence was emplaced east of all the previous plutons straddling the Sierra crest. This sequence is composed of porphyritic granodiorite, forming a nested elongated body at least 1200 km^2 in size. The U-Pb ages from the outer Paradise pluton (samples 21-23) range from 84 to 86 m.y. which is slightly older than that of the inner Whitney pluton, 83 m.y. (sample 49), which is in good agreement with K-Ar dates from the body [Evernden and Kistler, 1970]. Granodiorite of the Lone Pine pluton (87 m.y., sample 50) 15 km west of Lone Pine was emplaced on the east of the Whitney pluton; it, paired with the Sugarloaf pluton west of the Whitney Pluton (88 m.y., sample 48), may form the outer shell of the Paradise-Whitney sequence.

A few samples 70 km west of Lone Pine (34, 56-58) yield slightly discordant U-Pb ages of about 98 m.y. and probably represent the western boundary of the Late Cretaceous belt. A sample (59) from west of the Kern Canyon fault yields discordant U-Pb ages with $^{206}Pb/^{238}U$ ages ranging from 83 to 95 m.y. for three analyses. This discordant age may be result from intrusion of the large Paradise-Whitney sequence to the east. Quartz monzonite of the Alabama Hills (sample 51) just west of Lone Pine yields a concordant age of 85 m.y. (fine zircons) and discordant ages with the $^{206}Pb/^{238}U$ age of 87 m.y. (medium zircons).

Granitoid sequences of the Late Cretaceous belt can be compared with those reported by Kistler et al. [1965], Evernden and Kistler [1970], and Stern et al. [1981]. They also find an eastward progression of emplacement ages. A few granitic plutons in the White Inyo Mountains, immediately east of the Sierra Nevada, are considered satellites of the Sierra Nevada batholith. These plutons generally give Late Cretaceous ages (~85 m.y.) A few examples are the quartz monzonite of the Alabama Hills, Papoose Flat pluton [Evernden and Kistler, 1970], and the Pellisier Flat pluton [Stern et al., 1981].

The last intrusive activity in the Sierra Nevada during the Cretaceous was probably marked by the intrusion of a few prominent silicic dikes. For example, a dike (sample 12) from the Brush Canyon pluton 58 km west of Independence yields concordant U-Pb ages of 86 m.y.; the Golden Bear granite porphyry dike (sample 64) on the east Sierran escarpment 9 km west-southwest of Independence yields a concordant U-Pb age of 80 m.y. A granite porphyry dike (sample 65) in the North Argus Range 30 km northeast of Coso Junction may also belong to this dike activity. The U-Pb age of this dike is discordant with a $^{206}Pb/^{238}U$ age of 88 m.y.

Sphene U-Pb Ages

Seven sphene U-Pb ages were determined for samples in which zircon U-Pb ages were also measured. The results shown in Table 1 indicate that (1) most sphene U-Pb ages are younger than the zircon U-Pb age; for example, Lookout Peak (sample 16), North Dome (18), Woods Lake mass of Tinemaha granodiorite (26), Lodgepole (41), and (2) a few sphene U-Pb ages agree within error (±3 m.y.) with the zircon U-Pb age, for example, Paradise (21), Weaver Lake (45), Big Meadow (43). In the case of the Lodgepole pluton (sample 41), the sphene U-Pb age is concordant (96 m.y.) but is 19 m.y. younger than the zircon U-Pb age (115 m.y.). The Lodgepole pluton was intruded by the Giant Forest-alaskite sequence on the west. The sphene U-Pb age of the Lodgepole pluton agrees with the youngest U-Pb age of the Giant Forest-alaskite sequence (97 m.y.), suggesting resetting of the sphene U-Pb age by the intrusion of this later plutonic sequence. Recrystallization of sphene is indicated by its occurrence intergrown with biotite. Some of the sphene might be secondary, generated by the breakdown of biotite. The sphene U-Pb age determinations on granitoids of the Sierra Nevada batholith show the potential of dating the intrusive age of a pluton or of recording the last thermal event which caused the sphene U-Pb to become an open system or of dating the time when new sphene crystals were formed.

Comparison between U-Pb and K-Ar Ages

A direct comparison between U-Pb and K-Ar ages cannot be made because none of the samples in this study have been analyzed for K-Ar ages. However, many K-Ar ages are available on granitoids in the vicinity of our sample localities. A few comparisons have been discussed in the previous sections. The zircon ^{238}U-^{206}Pb ages are: (1) equal to (sample 49), (2) older than (28), or (3) younger than (29, 68, 73) the oldest K-Ar ages (mostly hornblende) in that area. In the last case the U-Pb ages are very discordant (except sample 77) with $^{207}Pb/^{206}Pb$ ages equal to or older than the K-Ar ages. In the Peninsular Ranges batholith, Silver et al. [1979] also had difficulty explaining why some K-Ar ages reported by Krummenacher et al. [1975] are older than concordant zircon U-Pb ages in the same area. Some possible explanations are (1) sampling problems (2) inheritance of initial radiogenic argon [Silver et al., 1979], or later argon gain, and (3) potassium loss. Certainly this kind of discrepancy requires more detailed study.

K-Ar ages for a series of samples from a west-east traverse across the Sierra Nevada batholith (Figure 2) were determined by Evernden and Kistler [1970]. Both zircon U-Pb and K-Ar ages for samples in this area are projected onto the reference line D-D' (Figure 3) which is normal to the elongation of plutons. The profile shown in Figure 9 permits a general comparison between U-Pb and K-Ar ages as follows:

1. Most K-Ar ages are equal to or younger than U-Pb ages at a corresponding segment of the traverse.
2. Most hornblende K-Ar ages are older than the paired biotite K-Ar ages.

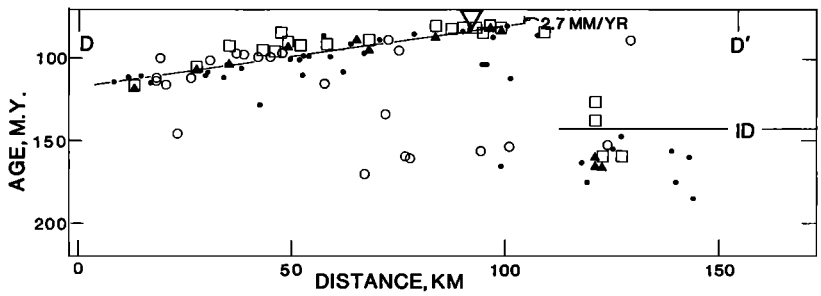

Fig. 9. Profiles of ^{238}U-^{206}Pb and ^{40}K-^{40}Ar ages in granitoid rocks projected on the W-E traverse D-D'(Figure 3) across the central Sierra Nevada batholith. Filled circles, concordant zircon U-Pb ages; open circles, discordant ages from this work (Table 2). Open squares, biotite K-Ar ages; closed triangles, hornblende K-Ar ages from Evernden and Kistler (1970). Large triangle, crest of Sierra Nevada; ID, age of Independence dike swarm.

3. The field of Cretaceous K-Ar ages is more restricted than that of Cretaceous U-Pb ages.

Features 1 and 2 are internally consistent with the respective blocking temperatures of the analyzed minerals. In the Cretaceous granitoids the differences between paired K-Ar ages are small (1-7 m.y.), indicating that cooling was sufficiently rapid after initial emplacement or later heating. On the other hand, in some Jurassic granitoids, the difference is as high as 33 m.y., indicating a complicated thermal history.

Excellent agreement between the U-Pb and K-Ar ages exists for samples from the western foothills (~115 m.y.) or the eastern Sierran crest area (~82 m.y.). Granitoids in the crest area represent the youngest intrusive event, and those in the foothills were probably well shielded by large volumes of granitoid rocks, mostly of the same age.

Larger differences between U-Pb and K-Ar ages appear at the neighborhood of the GFA sequence (~99 m.y.) where the K-Ar ages (mostly biotite) on samples from just south of this sequence are 5 to 15 m.y. younger. One possible explanation is that these K-Ar ages were partly reset by the intrusion of the nearby large Whitney-Paradise sequence (83-85 m.y.). In this segment of the traverse, just to the north of the GFA sequence, a few samples from the Kings Canyon area give U-Pb ages of ~110 m.y., which are close to that in the western foothills. These older U-Pb ages from the Kings Canyon area and several others (100-165 m.y.) from the eastern Sierra region are not found in

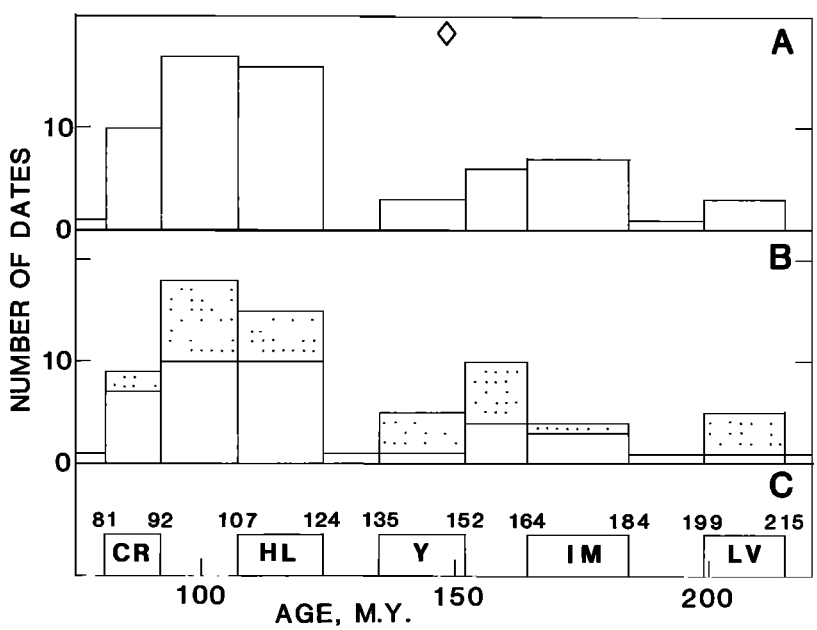

Fig. 10. Comparison of U-Pb and K-Ar age data for Sierra Nevada batholith. A, $^{206}Pb/^{238}U$ ages from Stern et al. (1981). B, Preferred intrusive ages of granitic plutons from this study (Table 2); dotted ages are discordant. C, Five intrusive epochs of Evernden and Kistler adjusted to new decay constants (Steiger and Jager, 1977) as follows: CR, Cathedral Range; HL, Huntington Lake; Y, Yosemite; IM, Inyo Mountains; and LV, Lee Vining. Diamond represents the period of intrusion of the Independence dike swarm.

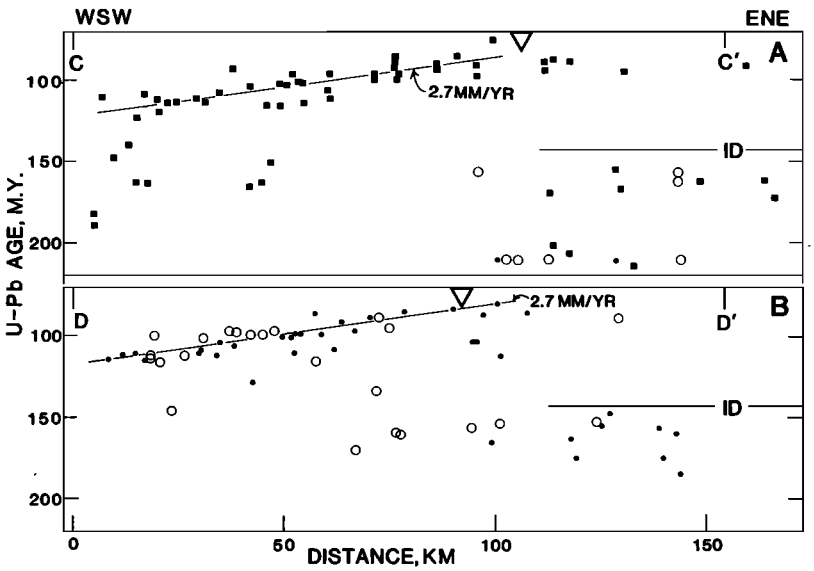

Fig. 11. Pb-U ages of granitic rocks projected onto lines C-C' and D-D' parallel to migration of plutonism as shown in Figure 3. (a) Dates between 36° and 37° latitude: solid squares, ages from Stern et al. [1981]; solid circles, concordant ages from this report (Table 2); open circles, discordant ages from this report. (b) Dates between 37° and 38° latitude. ID, age of Independence dikes; triangles, crest of Sierra Nevada.

the K-Ar ages and apparently do not occur to the south or were not sampled.

The age distribution of the dated granitic plutons from this study and other studies in the area of Figure 3 are summarized in Figure 10. The five intrusive epochs of Evernden and Kistler [1970] are shown for comparison and clearly occur in the same overall age range (80-220 m.y.). However, the U-Pb ages of this study and those of Stern et al. [1981] do not differentiate the five intrusive epochs proposed by Evernden and Kistler [1970]. In particular major intrusions about 100 m.y. old defined by the U-Pb method fill the gap between the Cathedral Range and Huntington Lake K-Ar epochs. Likewise, several U-Pb ages of about 160 m.y. fill the gap between the Yosemite and Inyo Montains K-Ar epochs. Only one age (sample 9) in the western Sierra occurs in the gap between the Huntington Lake and Yosemite epoch, but this gap probably reflects the period of no eastern plutonism between the Independence dike intrusion and the major Cretaceous plutonism. Although plutons dated by the U-Pb method occur in all of the proposed K-Ar epochs, the substantial proportion that occur between them causes us to question the significance of the five epochs of plutonism defined by the K-Ar method.

Eastern Time Gap in Plutonism and Independence Dike Swarm

Uranium-lead dating of granitic rocks east of the crest of the Sierra Nevada (Figure 11) indicate three general groups of ages: Triassic (202-215 m.y.), Jurassic (149-185 m.y.), and Cretaceous (80-112 m.y.). The age gap of 37 m.y. between Jurassic and Cretaceous pluton emplacement is increased to 54 m.y. if the three Early Cretaceous plutons just east of the Sierra Crest (Figure 11b) are excluded. This gap is filled toward the west with the appearance of progressively older Cretaceous plutons as well as Late Jurassic plutons in the western Sierra.

The termination of eastern Jurassic plutonism was followed directly by emplacement of the calc-alkalic Independence dike swarm about 148 m.y. ago (Figure 11). The dikes intrude roughly parallel to the axis of the Triassic-Jurassic belt east of the Sierra Nevada for a distance of 350 km (Figure 8). The large extent of the dike swarm indicates that it was intruded into a fracture system resulting from regional extension.

At roughly the period of this regional extension east of the Sierra Nevada, Jurassic and older volcanic and sedimentary rocks of the western Sierra Nevada were undergoing metamorphism and deformation during the Nevadan orogeny. Stern et al. [1981] suggest that the Nevadan orogeny occurred between 149 and 140 m.y. ago based on fossils within the Mariposa Formation (generally considered to be the youngest formation affected by the orogeny) and Pb-U ages of the crosscutting Guadalupe igneous complex. The regional extension east of the Sierra Nevada reflected by emplacement of the dike swarm could have resulted from a change in the regional stress pattern accompanying the Nevadan orogeny.

Migration of Cretaceous Plutonism

Uranium-lead dates of Cretaceous plutons in the Sierra Nevada define a steady east-northeast migration of granitic intrusion during the period of about 120-80 m.y. ago. Plots of dated samples along lines parallel to the direction of migration (normal to pluton elongation) indicate that the migration between both 37°-38° and 36°-37° north latitude was 2.7 mm/yr (Figure 11).

Similar rates have been determined by Krummenacher et al. [1975] in the Cretaceous batholith of Baja California. At 32° north latitude they found that the distance between biotite K-Ar gradients of 115 and 80 m.y. is 123 km and between hornblende K-Ar gradients of 110 and 80 m.y. is 95 km. These data indicate an eastward migration of Cretaceous plutonism of 3.5 and 3.2 mm/yr, respectively. However, Silver et al. [1979], based on their zircon U-Pb ages from granitoids in the Peninsular Ranges batholith, defined two distinct belts of plutons: an older (105 to 120+ m.y.) western static volcano-plutonic arc and a younger (105-89 m.y.) migrating plutonic arc. They indicate an eastward migration of the eastern belt of 7-8 mm/yr, but a straight line through all the data points indicates an average rate of 4-5 mm/yr [Silver et al., 1979, Figure 3].

The rate of migration of Sierra Nevada plutonism during 40 m.y. in the Cretaceous is an order of magnitude less than the relative motion of lithospheric plates and indicates a remarkably steady rate of subduction during that period. The fact that subduction conditions were so stable over such a prolonged period could account for the great volume of the Cretaceous batholith. The eastward migration of plutonism was accompanied by simultaneous westward migration of the trench-slope break and increase in width of the Great Valley forearc basin between the trench and the Sierra Nevada [Ingersoll, 1978]. These relations suggest that as Cretaceous subduction matured a general uplift of the lithosphere occurred. The present study does not provide new constraints on the cause of the eastern sweep of Cretaceous plutonism from 120-80 m.y. ago. It probably resulted either from increasing depth of parent magma generation along a steady, rather steeply dipping subduction system [Keith, 1978] or from a general flattening of an original steeply dipping system [Coney and Reynolds, 1977]. The bulk compositional gradient along this part of the continental margin lithosphere makes assignment of a process speculative.

Sierran igneous activity culminated in the intrusion of giant plutons near the crest of the range about 80 m.y. ago, as shown by the youngest U-Pb ages of granitic rocks in the map area (Figure 3). This abrupt termination of plutonism has been inferred to result from accelerated convergence between the American and eastern Pacific plates [Coney, 1972]. Beginning at 80 m.y. ago igneous activity moved eastward at a rate an order of magnitude greater than during the previous 40 m.y. probably as a result of this inferred increased convergence and rapid flattening of the subduction system [Coney and Reynolds, 1977; Keith, 1978; Lipman, 1980]. Consequently, smaller plutons, and no major batholithic belt, were produced to the east.

Conclusions

The results of 140 U-Pb mineral ages on 82 granitic masses in the central Sierra Nevada can be summarized as follows:

1. The U-Pb ages reported here are consistent with and extend those reported by Stern et al. [1981] in the central Sierra Nevada to the north of this study area. The new results do not differentiate the five cyclic epochs of plutonism in California and adjacent areas proposed by Evernden and Kistler [1970] and Kistler et al. [1971] on the basis of K-Ar dating and a few Rb-Sr whole rock isochrons.

2. The age distribution of Mesozoic granitic rocks studied in this work is in general agreement with that reported by Evernden and Kistler [1970], Kistler et al. [1971], and Kistler [1974]. Triassic plutons are localized on the east side of the batholith. Jurassic plutons occur south and east of the Triassic plutons east of the Sierra Nevada, form isolated masses within the Cretaceous batholith, and occur in the western Sierra foothills principally north of 37° north latitude.

3. Following emplacement of the Jurassic plutons east of the Sierra Nevada, no granitic intrusion occurred for 37 m.y. The Late Jurassic (148 m.y.) Independence dike swarm was intruded in a zone 350 km long and 30 km wide at the beginning of this period of no granite plutonism. The dike injection probably represents a period of crustal extension at the eastern margin of the Sierra Nevada.

4. Intrusion of Cretaceous granitic plutons in large volume began about 120 m.y. ago in the western Sierra Nevada and migrated relatively steadily eastward to the area of the present Sierra crest at a rate of 2.7 mm/yr. This slow migration may result either from parent magma generation at successively deeper levels or from a general flattening of the subduction system. The abrupt termination of Sierran plutonism 80 m.y. ago may have resulted from an increased rate of convergence of the American and eastern Pacific plates and rapid flattening of the subduction system.

5. U-Pb ages (99±3 m.y.) determined from a group of nested plutons, the Giant Forest-alaskite sequence, indicate that the time of emplacement of the entire sequence is relatively short (1-2 m.y.), and cooling of the plutonic complex took about 3 m.y. from the margin toward the center.

6. A mafic inclusion from the Giant Forest-alaskite sequence yields concordant U-Pb ages which fall within the range of age of the host pluton, indicating that the mafic inclusion and the host granodiorite were derived from a common source or that the mafic inclusion was totally equilibrated with the granodioritic magma.

7. Comparison among isotopic ages determined by different methods such as zircon U-Pb, sphene U-Pb, hornblende K-Ar and biotite K-Ar suggests that the zircon U-Pb ages can generally approximate the emplacement age of a pluton. However, some plutons probably contain 'inherited' or 'entrained' old zircons, and the zircons of some samples are disturbed by younger thermal and metamorphic events.

TABLE A1. Sample Localities and Descriptions

Sample	Field	Latitude North	Longitude West	Descriptions
1	W10	36°43.1'	119°21.4'	Quartz diorite, Hwy. 180, 2.4 km NNE of Granite Hill
2	W12	36°43.3'	119°18.4'	Quartz diorite, Hwy. 180, 4 km E of Cove Ave. intersection
3	W22	36°43.5'	119°17.5'	Quartz diorite, on Hwy. 180, 3 km W of Squaw Valley Santa Rita Mission
4	W21	36°45.5'	119°14.3'	Gabbro, Pine Flat road, 1 km N of Hwy. 180
5	W5	36°44.9'	119°13.7'	Quartz diorite, Hwy. 180 E of Squaw Valley and 1.9 km W of Mill Creek bridge; includes some metasedimentary rock (biotite schist) and migmatite
6	W4	36°46.2'	119°7.2'	Quartz diorite, Hwy. 180, 3.2 km N of Dunlap
7	W3	36°44.8'	119°3.6'	Quartz diorite, Hwy. 180, N of Black Oak Flat, near Snowline Lodge
8	W2	36°43.6'	119°0.5'	Garnet-biotite-muscovite-silimanite-alaskite, Hwy. 180, 2.4 km W of Sequoia Lake
9	W6	36°43.3'	118°58.2'	Quartz monzonite, Big Stump picnic area
10	KC11	36°49.4'	118°52.9'	Aplite dike in Yucca Point Pluton (1), Hwy. 180
11	KC6	36°49.8'	118°52.2'	Quartz diorite of the Yucca Point pluton (1), Hwy. 180, near Yucca Point
12	KC19	36°49.7'	118°51.5'	Dike from quartz monzonite of the Brush Canyon pluton (1) cutting metaquartzite, Hwy. 180, 1.2 km E of Yucca Point
13	KC18	36°48.5'	118°47.9'	Granodiorite of the Tombstone Creek pluton (1), Hwy. 180, E of metasiltstone unit of the Boyden Cave pendant
14	KC5	36°48.5'	118°47.5'	Granodiorite of the Tombstone Creek pluton (1), Hwy. 180, W of metavolcanic roof pendant
15	KC16	36°48.6'	118°45.6'	Granodiorite of the Lightning Creek pluton (1), Hwy. 180
16	KC2	36°48.2'	118°43.0	Granodiorite of the Lookout Peak pluton (1), Hwy. 180
17	KC15	36°47.8'	118°40.5'	Granodiorite of the Lookout Peak pluton (1), N of Cedar Grove Campground
18	68M91	36°49.7'	118°40.8'	Granodiorite of the North Dome pluton (1)
19	KC14	36°46.8'	118°37.1'	Alaskitic aplite of the North Mountain stock (2),
20	KC22			Roaring River Falls, KC22 collected 10 m away from KC14
21	57N73	36°50.0'	118°36.0'	Granodiorite of the Paradise pluton, summit of Mt. Hutchings (2, 3)
22	KC13	36°47.9'	118°34.3'	Granodiorite of the Paradise pluton (2, 3), about 1.6 km E of Zumwalt Meadow
23	KC20	36°48.8'	118°33.1'	Granodiorite of the Paradise pluton (2, 3), W side of Mist Falls
24	OW4	36°46.2'	118°20.9'	Alaskitic granite of the Bullfrog pluton (3), N shore of Little Pothole Lake, W of Onion Valley
25	OW34	36°46.6'	118°19.9'	Quartz monzonite of the Dragon Pluton (3), roadcut at Onion Valley
26	OW6	36°47.1'	118°18.9'	Granodiorite of the Woods Lake mass of Tinemaha granodiorite (3), roadcut 1.6 km E of Onion Valley
27	OW7	36°47.6'	118°18.2'	Granite of the Independence pluton (3), roadcut at Seven Pines
28	OW19	36°54.3'	118°9.7'	Granodiorite of the Santa Rita Flat pluton (4), about 4.8 km SE of Jack Black mine
29	E-27-9	36°50.7'	118°3.6'	Quartz monzonite of the Paiute Monument pluton (4), dirt road about 1.5 km NE of Whiteside mine
30	W24	36°42.5'	119°15.5'	Quartz diorite, Sand Creek road 2.4 km S of Ruth Hill road
31	W26	36°39.9'	119°13.1'	Quartz diorite, paved road W of BM878, E of Sand Creek, 0.8 km N of county line in Fresno County.
32	W16	36°34.5'	119°09.3'	Quartz diorite, paved road 0.4 km E of Moore Creek road
33	W18	36°37.0'	119°02.1'	Quartz diorite, W of BM2753, 0.8 km N of Pippin Flat
34	W19	36°40.1'	118°58.8'	Quartz diorite, 2.4 km NW of Hartland
35	SQ57	36°44.2'	118°53.6'	Mafic inclusion in the Giant Forest pluton (5), road 2.4 km N of Quail Flat
36	SQ9	36°38.9'	118°49.5'	Granodiorite of the Giant Forest pluton (5), Hwy. 198, near Lost Grove
37	SQ22	36°36.3'	118°44.3'	Aplite dike in the Giant Forest pluton (5), Hwy. 198, 1.6 km W of Lodgepole Campground.

TABLE A1. (continued)

Sample	Field	Latitude North	Longitude West	Descriptions
38	SQ75	36°34.9'	118°45.2'	Granodiorite of the Giant Forest pluton (5), Hwy. 198, near General Sherman Tree
39	SQ7	36°33.4'	118°46.3'	Granodiorite of the Giant Forest pluton (5), Hwy. 198, 1.6 km NW of Moro Rock
40	SQ5	36°31.0'	118°47.2'	Granodiorite of the Giant Forest pluton (5), Hwy. 198, 0.8 km W of the Sequoia roof pendant
41	SQ8	36°36.2'	118°43.2'	Granite of the Lodgepole pluton (5), at Lodgepole Campground, 0.4 km N of Kaweah River
42	SQ12	36°40.0'	118°50.1'	Granodiorite of the Big Meadow pluton (5), Hwy. 198, near Stoney Creek Campground, 0.4 km W of Stony Creek
43	SQ48	36°43.4'	118°48.4'	Granodiorite of the Big Meadow pluton (5), about 0.4 km E of Heart Meadow Campground N of Big Meadow Creek
44	SQ13	36°38.4'	118°48.3'	Quartz monzonite of the Weaver Lake pluton (5), Hwy. 198, 0.8 km NE of Dorst Campground
45	SQ46	36°43.8'	118°47.3'	Quartz monzonite of the Weaver Lake pluton (5), about 1.9 km E of Heart Meadow Campground, 1.6 km W of Boulder Creek
46	SQ61	36°41.0'	118°50.0'	Alaskite, within the Big Meadow pluton (5), 1.2 km W of Stoney Creek 1.6 km E of Hwy. 198
47	SQ67	36°43.1'	118°43.0'	Granodiorite of the Mitchell Peak pluton (2), 1 km S of Mitchell Peak Lookout
48	68M15	36°45.2'	118°36.8'	Granodiorite of Sugarloaf, 3.2 km S of Roaring River Falls (2)
49	OW40	36°33.7'	118°17.5'	Whitney porphyritic granodiorite (6), 1 km S of Mt. Whitney, at trail close to BM 13480
50	OW41	36°35.7'	118°13.2'	Granodiorite of Lone Pine pluton (6), road 1.6 km E of Whitney Portal
51	E27-3	36°35.2'	118°6.7'	Quartz monzonite of Alabama Hills, road about 3.2 km N of Tuttle Creek, 1.6 km S of Lone Pine Creek
52	W29	36°24.3'	119°3.2'	Quartz diorite, 2.4 km E of Woodlake, just E of town of Naranjo
53	W30	36°23.6'	118°57.8'	Quartz diorite, S shore of Lake Kaweah on Hwy. 198, 1 km W of campground turnoff
54	W31	36°24.7'	118°56.2'	Quartz diorite, E arm of Lake Kaweah, 1.6 km N of Tharps Peak, Hwy. 198 at turnoff to marina road
55	W32	36°26.4'	118°54.2'	Quartz diorite across from Three Rivers post office, Hwy. 198
56	W34	36°27.5'	118°52.3'	Quartz diorite, Hwy. 198, W of Salt Creek bridge, E end of Three Rivers, and W of BM1030
57	SQ3	36°30.1'	118°48.5'	Granite of the Cactus Point pluton (5), Hwy. 180, 1.6 km NE of Ash Mountain Park Headquarters
58	SQ15	36°30.8'	118°48.2'	Quartz diorite of the Potwisha pluton (5), Hwy. 180, 0.4 km W of Potwisha Campground
59	6-124	36°32.5'	118°28.6'	Granite of Mt. Kaweah (6) 1.6 km N of Mt. Kaweah
60	7-19	36°26.6'	118°23.9'	Porphyritic granodiorite 1 km E of Kern River, opposite Big Arroyo; sheared and cut by mafic dikes
61	77-7	36°25.4'	118°23.6'	Porphyritic granodiorite 1.6 km E of Kern River opposite Rattlesnake Creek; cut by many sheared mafic dikes
62	7-51	36°12.2'	118°25.2'	Coarse-grained granodiorite 0.4 km SE of Trout Meadow Guard Station on E side of Kern Canyon fault, generally cut by mafic dikes
63	8-38a	36°59.3'	118°23.9'	Alaskitic quartz monzonite of Red Mountain Creek pluton (3), 1.8 km SE of Cardinal Mountain, cut by mafic dikes
64	7-55	36°45.2'	118°16.6'	Granite porphyry Golden Bear Dike (3, 6), SE corner of Mt. Pinchot quadrangle, 6,400 ft ridge top N of Symmes Creek
65	8-124-3	36°12.5'	117°39.5'	Granite porphyry dike, 26 km E of Haiwee Reservoir, northern Coso Mountains
66	8-54	36°50.1'	118°23.0'	Granodiorite of White Fork pluton 1.3 km NE of Diamond Peak (3)
67	MA2	37°53.6'	118°50.8'	Porphyritic granodiorite of Benton Range, Gaspipe Spring, 11 km SE Mono Lake, 0.4 km W of BM7974, Hwy. 120, cut by mafic dike

TABLE A1. (continued)

Sample	Field	Latitude North	Longitude West	Descriptions
68	MA5	37°51.6'	118°37.8'	Porphyritic granodiorite of Benton Range, Hwy. 120, S of BM6642, 4.8 km W of S end Antelope Lake
69	MA7	37°39.1'	118°34.7'	Rhyolite dike cutting quartz-sericite hornfels, 0.4 km E of Moran Spring on road NE of peak 7489 (12)
70	MA9	37°39.0'	118°32.3'	Porphyritic granodiorite of Benton Range (12), N of ridge crest on road E of Chidago Flat, 1.6 km SE of Kings Mill site
71	MA16	37°45.8'	119°7.5'	Granite dike 30-40 ft thick cutting quartz monzonite of Lee Vining Canyon (8), tramway 0.8 km S of Silver Lake
72	MA17	37°45.8'	119°7.4'	Quartz monzonite of Lee Vining Canyon (8) down tramway from MA16
73	MA1	37°57.1'	119°13.5'	Quartz monzonite of Lee Vining Canyon (8), Tioga Road, 1.8 km E of Tioga Peak
74	OW2	37°22.8'	118°40.7'	Quartz monzonite of Tungsten Hills (9), N of Sheelite (site), Pine Creek
75	MG6-24	37°7.9'	118°44.4'	Sheared granodiorite of Goddard pendant (11), 0.5 km W of Davis Lake
76	F1-57	36°36.2'	117°58.3'	Quartz monzonite of Long John pluton (10), N of Owens Lake
77	02-26	36°16.4'	117°34.7'	Monzonite of Darwin stock (10), road 1 km E of Darwin
78	COSO-1	36°15.1'	117°35.3'	Quartz monzonite of Coso pluton (10), road 3.2 km S of Darwin
79	GRB	36°5.8'	117°26.5'	Granite of Bendire Canyon in Bendire Canyon (10)
80	JMP	36°01.6'	117°25.5'	Quartz monzonite of Maturango Peak (10) in Shepherd Canyon
81	OW11	35°39.8'	117°25.7'	Quartz monzonite of Southern Argus Range (10) at roadcut in Poison Canyon
82	OW37	35°38.8'	117°25.1'	Granodiorite of Eastern Spangler Hills (10), 0.8 km S of road at Poison Canyon

Numbers in parentheses refer to references of pluton names: (1) Moore et al. [1972], (2) Moore [1978], (3) Moore [1963], (4) Ross [1969], (5) Ross [1958], (6) Moore [1981], (7) Stern et al. [1981], (8) Kistler [1966a, b], (9) Bateman [1961], (10) Dunne et al. [1978], (11) Bateman and Moore [1965], (12) Rinehart and Ross [1957].

Acknowledgement. This report is based on parts of J. H. Chen's Ph. D. dissertation. One of us (JHC) would like to thank G. R. Tilton for his advice and support through this work. We thank C. R. Bacon, P. C. Bateman, C. A. Hopson, R. W. Kistler, J. M. Mattinson, Jason Saleeby, R. W. Tabor, M. Grünenfelder, and L. T. Silver for useful discussions and reviews. The help of officials of Sequoia and Kings Canyon National Park for granting permits to collect rocks in the park area is appreciated.

References

Armstrong, R. L., and J. Suppe, Potassium-argon geochronometry of Mesozoic igneous rocks in Nevada, Utah, and southern California, Geol. Soc. Am. Bull., 84, 1375-1392, 1973.

Bateman, P. C., Granitic formations in the east-central Sierra Nevada near Bishop, California, Geol. Soc. Am. Bull., 72, 1521-1537, 1961.

Bateman, P. C., and F. C. W. Dodge, Variations of major chemical constituents across the central Sierra Nevada batholith, Geol. Soc. Am. Bull., 81, 409-420, 1970.

Bateman, P. C., and J. P. Eaton, Sierra Nevada batholith, Science, 158, 1407-1417, 1967.

Bateman, P. C., and J. G. Moore, Geologic map of the Mount Goddard quadrangle, Fresno and Inyo counties, California, U.S. Geol. Surv. Geol. Quadrangle Map, GQ-429, 1965.

Bateman, P. C., and C. Wahrhaftig, Geology of the Sierra Nevada, in Geology of Northern California, Bull. Calif, Div. Mines Geol., 90, 107-172, 1966.

Bateman, P. C., L. D. Clark, N. K. Huber, J. G. Moore, and C. D. Rinehart, The Sierra Nevada batholith--A synthesis of recent work across the central part, U.S. Geol. Surv. Prof. Pap., 414-D, D1-D46, 1963.

Catanzaro, E. J., T. J. Murphy, W. R. Shields, and E. L. Garner, Absolute isotopic ratios of common equal-atom and radiogenic lead isotopic standards, J. Res. Natl. Bur. Stand., 72A, 261-267, 1968.

Chen, J. H., Uranium-lead isotopic ages from the southern Sierra Nevada batholith and adjacent areas, California, Ph.D. thesis, 138 pp., Univ. of Calif., Santa Barbara, 1977.

Chen, J. H., and J. G. Moore, The Late Jurassic

Independence dike swarm in eastern California, Geology, 7, 129-133, 1979.

Chen, J. H., and G. R. Tilton, Lead and strontium isotopic studies of the southern Sierra Nevada batholith, California, Geol. Soc. Am. Abstr. Programs, 10, 99-100, 1978

Coney, P. J., Cordilleran tectonics and North American plate motion, Am. J. Sci., 272, 603-628, 1972.

Coney, P. J., and S. J. Reynolds, Cordilleran Benioff zones, Nature, 270, 403-405, 1977.

Crowder, D. F., E. H. McKee, D. C. Ross, and K. B. Krauskopf, Granitic rocks of the White Mountain area, California-Nevada: Age and regional significance, Geol. Soc. Am. Bull., 84, 285-296, 1973.

Dodge, F. C. W., and R. E. Mays, Rare-earth element fractionation in accessory minerals: central Sierra Nevada batholith, U.S. Geol Surv. Prof. Pap. 800-D, D165-D168, 1972.

Doe, B. R., and M. H. Delevaux, Variations in lead-isotopic compositions in Mesozoic granitic rocks of California: a preliminary investigation, Geol. Soc. Am. Bull., 84, 3513-3526, 1973.

Dunne, G. C., R. M. Gulliver, and A. G. Sylvester, Mesozoic evolution of rocks of the White, Inyo, Argus, and Slate ranges, eastern California, in Mesozoic Paleogeography of the Western United States, edited by D. G. Howell and K. McDougall, p. 189-207, Society of Economic Paleontologists and Mineralogists, Pacific Section, Pacific Coast Paleogeography Symposium 2, Los Angeles, 1978.

Evernden, J. F., and R. W. Kistler, Chronology of emplacement of Mesozoic batholithic complexes in California and western Nevada, U.S. Geol Surv. Prof. Pap., 623, 42 pp., 1970.

Hamilton, W., Mesozoic California and the underflow of Pacific mantle, Geol. Soc. Am. Bull., 80, p. 2409-2430, 1969.

Hart, S. R., The petrology and isotopic-mineral age relations of a contact zone in the Front Range, Colorado, J. Geology, 72, 5, 493-525, 1964.

Hart, S. R., G. L. Davis, R. H. Steiger, and G. R. Tilton, A comparison of the isotopic mineral age variations and petrologic changes induced by contact metamorphism, in Radiometric Dating for Geologists, edited by E. I. Hamilton and R. M. Farquhar, 73-110, Interscience, New York, 1968.

Ingersoll, R. V., Paleogeography and paleotectonics of the late Mesozoic forearc basin of northern and central California in Mesozoic Paleogeography of the Western United States, edited by D. G. Howell and K. McDougall, pp. 471-482, Society of Economic Paleontologists and Mineralogists, Pacific Section, Pacific Coast Paleogeography Symposium 2, Los Angeles, 1978.

Keith, S. B., Paleosubduction geometries inferred from Cretaceous and Tertiary magmatic patterns in southwestern North American, Geology, 6, 516-521, 1978.

Jaffey, A. H., K. F. Flynn, L. E. Glendenin, W. C. Bentley, and A. M. Essling, Precision measurement of half-lines and specific activities of ^{235}U and ^{238}U, Phys. Rev., C4, 1889-1906, 1971.

Kistler, R. W., Geological map of the Mono Craters quadrangle, Mono and Tuolumne Counties, California, scale 1:62,500, U.S. Geol. Surv. Geol. Quadrangle Map, GQ-462, 1966a.

Kistler, R. W., Structure and metamorphism in the Mono Craters quadrangle, Sierra Nevada, California, Geol. Soc. Am. Bull., 1221-E, E1-E53, 1966b.

Kistler R. W., Phanerozoic batholiths in western North America, Annu. Rev. Earth Planet. Sci., 2, 403-418, 1974.

Kistler R. W., and F. C. W. Dodge, Potassium-argon ages of coexisting minerals from pyroxene-bearing granitic rocks in the Sierra Nevada, California, J. Geophys. Res., 71 (8), 2157-2161, 1966.

Kistler, R. W., and Z. E. Peterman, Variations in Sr, Rb, K, Na, and initial Sr^{87}/Sr^{86} in Mesozoic granitic rocks and intruded wall rocks in central California, Geol. Soc. Am. Bull., 84, 3489-3512, 1973.

Kistler, R. W., P. C. Bateman, and W. W. Brannock, Isotopic ages of minerals from granitic rocks of the central Sierra Nevada and Inyo Mountains, California, Geol. Soc. Am. Bull., 76 (2), 155-164, 1965.

Kistler, R. W., J. F. Evernden, and H. R. Shaw, Sierra Nevada plutonic cycle, Part 1, Origin of composite granitic batholith, Geol. Soc. Am. Bull., 82, 853-868, 1971.

Krogh, T. E., A low-contamination method for hydrothermal decomposition of zircon and extraction of U and Pb for isotopic age determinations, Geochim. Cosmochim. Acta, 37, 485-494, 1973.

Krummenacher, D., R. G. Gastil, J. Bushee, and J. Doupont, K-Ar apparent ages, Peninsular Range batholith, southern California and Baja California, Geol. Soc. Am. Bull., 86, 760-768, 1975.

Lanphere, M. A., and B. L. Reed, Timing of Mesozoic and Cenozoic plutonic events in circum-Pacific North America, Geol. Soc. Am. Bull., 84, 3773-3782, 1973.

Lipman, P. W., Cenozoic volcanism in the western United States: implications for continental tectonics, in Studies in Geophysics: Continental Tectonics, pp. 161-174, National Academy of Sciences, Washington, 1980.

Mattinson, J. M., Anomalous isotopic composition of lead in young zircons, Yearbook Carnegie Inst. Washington, 72, 613-616, 1973.

Mattinson, J. M., Emplacement history of the Tatoosh volcanic-plutonic complex, Washington: Ages of zircons, Geol. Soc. Am. Bull., 88, 1509-1514, 1977.

Mattinson, J. M., Age, origin, and thermal histories of some plutonic rocks from the Salinian block of California, Contrib. Mineral. Petrol., 67, 233-245, 1978.

Moore, J. G., The quartz diorite boundary line in the western United States, J. Geol., 67, 189-210, 1959.

Moore, J. G., Geology of the Mount Pinchot quadrangle, southern Sierra Nevada, California, U.S. Geol. Surv. Bull., 1138, 152 pp., 1963.

Moore, J. G., Geologic map of the Marion Peak quadrangle, Fresno County, California, U.S. Geol. Surv. Geol. Quadrangle Map GQ-1399, 1978.

Moore, J. G., Geologic map of the Mount Whitney quadrangle, Inyo and Tulare counties, California, U.S. Geol. Surv. Geol. Quadrangle Map GQ-1545, 1981.

Moore, J. G., and E. du Bray, Mapped offset on the right lateral Kern Canyon fault, southern Sierra Nevada, California, Geology, 6, 205-208, 1978.

Moore, J. G., and C. A. Hopson, The Independence dike swarm in eastern California, Am. J. Sci., 259, 241-259, 1961.

Moore, J. G., L. Y. Marks, and H. W. Oliver, Mineral Resources of the High Sierra Primitive Area, California, U.S. Geol. Surv. Bull., 1371-A, 40 pp., 1972.

Pabst, A., Orientation of minerals in 'autolith,' Am. Mineral., 21, 68, 1936.

Rinehart, C. D., and D. C. Ross,. Geologic map of the Casa Diablo quadrangle, California, U.S. Geol. Surv. Quadrangle Map, GQ 99, 1957.

Ross, D. C., Igneous and metamorphic rocks of parts of Sequoia and Kings Canyon National parks, California, Spec. Rep. Calif. Div. Mines Geol., 53, 24, 1958.

Ross, D. C., Descriptive petrology of three large granitic bodies in the Inyo Mountains, California, U.S. Geol Surv. Prof. Pap., 01, 47 pp., 1969.

Saleeby, J. B., Polygenetic ophiolite belt of the California Sierra Nevada--geochronological and tectonostratigraphic development, J. Geophys. Res., 87, 1803-1824, 1982.

Saleeby, J. B., and W. D. Sharp, Chronology of the structural and petrologic development of the southwest Sierra Nevada foothills, California, Geol. Soc. Am. Bull., 91, 1416-1535, 1980.

Shaw, H. R., R. W. Kistler, and J. F. Evernden, Sierra Nevada plutonic cycle: II, Tidal energy and a hypothesis for orogenic-epirogenic periodicities, Geol. Soc. Am. Bull., 82, 869-896, 1971.

Silberman, M. L., and E. H. McKee, K-Ar ages of granitic plutons in north-central Nevada, Isochron/West, 71-1, 15-32, 1971a.

Silberman, M. L., and E. H. McKee, Period of plutonism in north-central Nevada, a section of gold-bearing deposits in north-central Nevada and south-western Idaho, Econ. Geol., 66 (1), 17-20, 1971b.

Silver, L. T., H. P. Taylor, Jr., and B. Chappell, Some petrological, geochemical and geochronological observations of the Peninsular Ranges batholith near the international border of U.S.A. and Mexico, in Mesozoic Crystalline Rocks: Peninsular Ranges Batholith and Pegmatites, Point Sal Ophiolite, Field Trip Guidebook, edited by P. L. Abbott and V. R. Todd, Geological Society of America, Boulder, Colo., 1979.

Smith, G. I., Large lateral displacement on Garlock fault, California, as measured from offset dike swarm, Am. Assoc. Pet. Geol. Bull., 46, 85-104, 1962.

Smith, J. G., E. H. McKee, D. B. Tatlock, and R. F. Marvin, Mesozoic granitic rocks in northwestern Nevada--A link between the Sierra Nevada and Idaho batholiths, Geol. Soc. Am. Bull., 82, 2933-2944, 1971.

Steiger, R. H., and E. Jager, Subcommission on geochronology: Convention on the use of decay constants in geo- and cosmochronology, Earth Planet. Sci. Lett., 36, 359-362, 1977.

Stern, T. W., P. C. Bateman, B. A. Morgan, M. F. Newell, and D. L. Peck, Isotopic U-Pb ages of zircon from the graitoids of the central Sierra Nevada, U.S. Geol Surv. Prof. Pap. 185, 17 pp., 1981.

Van Eysinga, F. W. B. (Compiler), Geological Time Table, 3rd ed., Elsevier, New York, 1975.

Wetherill, G. W., Discordant uranium-lead ages, I, Eos Trans. U., 37, no. 3, 320-326, 1956.

(Received May 12, 1981;
revised February 11, 1982;
accepted March 5, 1982.)